Technische Universität Berlin

Temporal comprehension in autonomous drone racing: infer navigation decisions from current and past raw sensor data with a recurrent convolutional neural network

Master Thesis

am Fachgebiet Agententechnologien in betrieblichen Anwendungen und der
Telekommunikation (AOT)
Prof. Dr.-Ing. habil. Sahin Albayrak
Fakultät IV Elektrotechnik und Informatik
Technische Universität Berlin

vorgelegt von
Friedrich Clemens Valentin Mangelsdorf

Betreuer: Dr. rer. nat Yuan Xu,
Gutachter: Prof. Dr.-Ing. habil. Sahin Albayrak
                   Prof. Dr. Odej Kao

Friedrich Clemens Valentin Mangelsdorf
Matrikelnummer: 356686

Erklärung der Urheberschaft

Ich erkläre hiermit an Eides statt, dass ich die vorliegende Arbeit ohne Hilfe Dritter und ohne Benutzung anderer als der angegebenen Hilfsmittel angefertigt habe; die aus fremden Quellen direkt oder indirekt übernommenen Gedanken sind als solche kenntlich gemacht. Die Arbeit wurde bisher in gleicher oder ähnlicher Form in keiner anderen Prüfungsbehörde vorgelegt und auch noch nicht veröffentlicht.

Ort, Datum   Unterschrift

Abstract

DELETEME: An abstract is a teaser for your work. You try to convince a reader that it is worth reading your work. Normally, it makes to structure you abstract in this way:

- one paragraph on the motivation to your topic

- one paragraph on what approach you have chosen

- and one paragraph on your results which may be presented in comparison to other approaches that try to solve the same or a similar problem.

Abstract should not exceed one page (aubrey's opinion)

Zusammenfassung

DELETEME: translate to German to Englisch or vice-versa.

Acknowledgements

Contents

List of Figures

List of Tables

Chapter 1

Introduction

DELETEME: for readability purpose, it makes sense to write a short paragraph on what the reader can expect in this chapter.

DELETEME: tipp: sometimes it makes sense to write the first chapter, the last chapter, and the abstracts at the end. In this case, it might be easier to argue towards your topic

1.1 Motivation

DELETEME: This section is very important since it argues why it is necessary to take care of the problem you are addressing in your work. One way to do this is coming from a very broad view on the problem to a very detailled one. This can be done by establishing a chain of statements that refer to each other until you reach your particular problem. Doing this, you really need to take care for citing every statement.

DELETEME: Example for a chain: Mobile communication gets increasingly popular in the world (CITE sales on mobile communication infrastruce, mobile phones, or increasing number of mobile phones contracts). $\rightarrow$ Especially smartphones, which represent the next generation cellular phone (CITE), get more and more used for communicating not only with other people but also for connecting to the Internet for using various services (CITE). $\rightarrow$ Smartphone are comprehensive cellular phones that provide additional functionality due to their increased connection and processing capabilities (CITE). $\rightarrow$ Most smartphones offer an online application store for adding software to the devices which helps the users to customize their devices according to their needs, e.g. Android Market[1]. $\rightarrow$ One problem about installing third-party software is that not all softwares try to help the user; $\rightarrow$ software with malicious intentions, so called malicious software (malware), can be a severe threat to smarptphone users. Some malwares delete files (EXAMPLE + CITE or footnote with URL) or even destroy devices

---

[1] http://market.android.com, visited on 05/08/2011
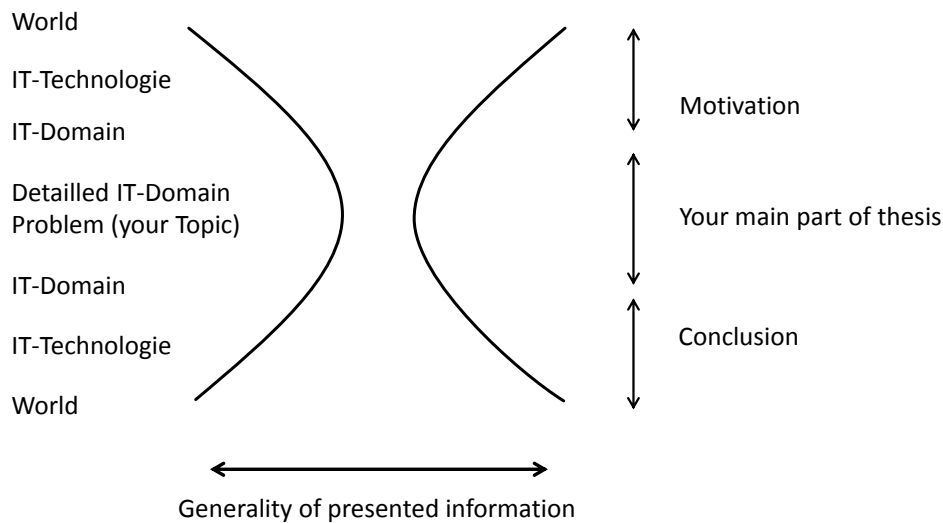
Figure 1.1: This images illustrates how generality of information could be handled in a thesis. In your motivation you should start from a very broad view on the topic. Then you should get more precise with every statement until you reach the actual problem you are addressing. You should do vice-versa in your conclusion, starting with the problem that you addressed and getting broader until you can write about the meaning of your results to the (IT-)world.

(EXAMPLE + CITE or footnote with URL). → More and more smartphone malwares appeared in the last years (CITE). → Signature-based approaches work efficiently on known malware (CITE) but face serious drawbacks regarding unknown malware. → Oberheide et al. [**?**] state that virus engines need an average time of 48 days until their databases get updated to be able to detect a certain unknown malware. → This in turn means that smartphone users stay unprotected for this time which can be seen as a severe threat. → Therefore, approaches are needed that are capable of detecting unknown malware for protecting the users against such threats. DELETEME: This example showed how one could argue that alternative approaches for malware detection is required. The length of the motivation depends on the topics handled and can of course be longer. The principle I am describing is also shown on Figure 1.1

1.2 Approach and Goals

DELETEME: In this section, you should cleary describe your approach that you are following in order to solve the underlaying problem of your thesis. Additionally, you should clearly state the goals of your work. This will not only help you supervizor

to understand what you are doing, it will also help you to be sure on which topic you should evaluate.

1.3   Structure of the Thesis

DELETEME: This section does not require eloquent writing. It is just a presentation of what you will handle in each chapter starting with Chapter 2.

DELETEME: Example: This thesis is structured as follows. In Chapter 2, we discuss essential background related to the thesis topic. (SOME MORE SENTENCES). Chapter 3 represents a detailled analysis of the problem that will be addressed. In particular, (SOME MORE SENTENCES). In Chapter 4, our solution is presented. This solution covers ... (SOME MORE SENTENCES). Chapter 5 evaluates our solution basing on our specified goals. (SOME MORE SENTENCES). In Chapter 6, we conclude. Chapter 6.3 gives additional related information on the topic of this thesis.

Chapter 2

Background

DELETEME: This chapter will cover all of your background information and related work. Background and related work are directly related to your thesis. Please do not place irrelevant content here which is a common mistake. Citing will be handled in the appendices.

DELETEME: Background represents underlaying knowledge that is required to understand your work. The expected knowledge level of your readers can be set to the one of a bachelor or master student who just finished his studies (depending on what kind of thesis you are writing). This means that you do not need to describe how computers work, unless your thesis topic is about this. Everything that an avarage alumni from your field of studies should now does not need to be described. It turn, background information that is very complex and content-wise very near to you problem, can be placed in the main parts. Everyting else should be written here. Note: it is important to connect each presented topic to your thesis. E.g. if you present the ISO/OSI layer model you should also write that this is needed to understand the protocols you plan to develop in the main parts.

DELETEME: Related work respresents results from work that handled the same or a similar problem that you are addressing. This work might have used a different approach or might not have been that successful. Finding a paper / work that solved your problem in the same way you were planning to do is not good and you should contact your supervizor for solving this issue. Again, each paper / work has to be connected to your approach: other papers might have not chosen an optimal solution; they might not have been taking care of essential aspects; they might have chosen a different approach and you believe, yours will work better ...

2.1 Topic 1

2.2 Topic 2

2.3 Gated recurrent unit

The artifical neural network (ANN) of the navigation method of this thesis integrates the PyTorch implementation[1] of the gated recurrent unit (GRU) with the objective to involve temporal comprehension in the navigation decision making. The GRU, published in 2014 by Cho et al. [3], is a variant of the ANN class of recurrent neural networks (RNN). This section shortly introduces the RNN class and justifies the design choice for the GRU in light of standard RNNs and the more prevalent long short-term memory (LSTM). Moreover, it provides an insight into the mechanisms of the GRU that make temporal comprehension available as well as the training process of the GRU.

RNNs contrasts with classical feedforward ANNs, which forward information exclusively towards subsequent layers, by featuring dynamic properties that stem from the implementation of feedback connections [11] (see fig. 2.1a). As previously infered states re-enter the network, the output of an RNN depends not only on the current but also on prior inputs. In this sense, an RNN is qualified to process and reason on entire sequences of data points. In case of time-series data, this can be interpreted as temporal comprehension and memory [12]. RNNs are trained on sequential data with backpropagation through time (BPTT) [18] which is basically the application of standard backpropagation (e.g., [19]) on the unfolded representation of the RNN. The unfolded representation exhibits a layer for each data point in the given input sequence (see figure 2.1b) and can be construed as a feedforward ANN that shares its trainable parameters across its layers. The longer the input sequences, the deeper the unfolded representation of an RNN becomes. The training of RNNs on long sequences is hence prone to the vanishing gradient problem [9], which manifests itself in the premature slowdown or standstill of the convergence of the RNN. As a result, it is difficult to teach standard RNNs to make connections to information of inputs deep in the past [1].

In 1997, Hochreiter and Schmidhuber [10] introduced the long short-term memory (LSTM), which is today's predominant [21] RNN variant. A standard LSTM unit (see, e.g., the PyTorch implementation[2]) recurrently maintains a cell and a hidden state, i.e., the unit re-inputs the fed back cell and hidden state outputted one sequential step before. Each sequential step, the unit additionally inputs the current element of the given input sequence. The LSTM unit implements three gating mechanism. A gating mechanism

---

[1]`https://pytorch.org/docs/stable/generated/torch.nn.GRU.html`, visited on 09/07/2022

[2]`https://pytorch.org/docs/stable/generated/torch.nn.LSTM.html`, visited on 03/07/2022

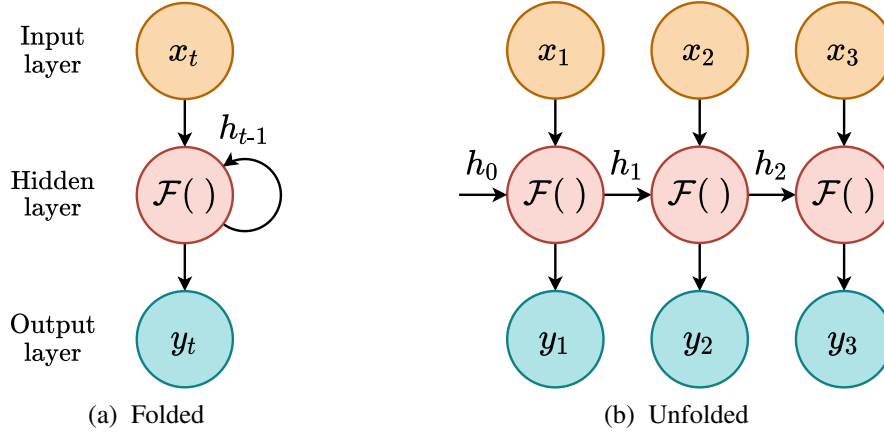| Input layer | Hidden layer | Output layer |

(a) Folded   (b) Unfolded

Figure 2.1: Folded schematic RNN with a single hidden layer that feeds the previous h_{t-1} (or initial h_0) state back to the inference at the current time step t and its time-unfolded representation when processing the input of a time-series consisting of the three data points $(x_i)_{i \in \{1,2,3\}}$.

is basically the Hadamard product of a state and a gate, which is a vector whose entries are between zero and one. The forget gate manipulates the information that are carried forward from the previous to the current cell state. The input gate controls the information that the the current cell state includes from the previous hidden state and the current element of the input sequence. Finally, its output gate regulates the information of the current cell state that are used to infer the current hidden state. All three gates are functions of the previous hidden state and the current element of the input sequence. This design makes the training of the LSTM essentially robust to the vanishing gradient problem [18]. As a result, teaching the LSTM to remember long-term dependencies within inputted sequences is considerably simplified in comparison to standard RNNs.

The GRU, which was proposed 17 years after the LSTM, can be seen as a lighter version of the LSTM. It refrains from the cell state and therewith the output gate of the LSTM and maintains only a hidden state with two gates. Therewith, the GRU has less trainable parameters than the LSTM and is less memory efficient during inference. Nevertheless, it preserves the robustness with respect to the "short-term memory problem" [12] due to the vanishing gradient affecting many standard RNNs. Various empirical studies show that the GRU, compared to the LSTM, performs equally well or even slightly better. Greff et al. [6] evaluated the "vanilla" LSTM and the GRU, among other LSTM variants, on speech and handwritten text recognition as well as music representation and could not detect substantial differences in performance. Chung et al. [4] applied LSTM and GRU on raw speech and polyphonic music data and empirically observed that both performed equally well. In the comparative study of Yin et al. [22],

the GRU slightly outperforms the LSTM on five of seven natural language processing tasks. In the field of algorithm learning, Kaiser and Sutskever [13] achieved notedly better results with a network based on GRU than with a network based on LSTM. In consideration of the above findings and the fact that the GRU has less trainable parameters and occupies less memory during inference, the GRU is chosen over the LSTM for deployment in the ANN module of the navigation method of this thesis.

Inference

The following presents the mathematics of a single GRU layer during inference in accordance with the PyTorch implementation[3]. This includes the GRU layer's two gating mechanisms as well as its computations of the candidate and the hidden state.

Without loss of generality, let the sequential data to be processed by the GRU layer be a batch of time series of data points

$$\left(\underline{x}_t \in \mathbb{R}^{N^{\text{in}}} \right)_{t \in \{1, \ldots, N^{\text{seq}}\}, i}, \quad i \in \left\{ 1, \ldots, N^{\text{batch}} \right\} \tag{2.1}$$

with the batch size N^{batch}, the sequence length N^{seq} and the dimensionality N^{in} of the data points. Let the initial batch of hidden states be

$$\underline{h}_{0,i} \in [-1, 1]^{N^{\text{hidden}}}, \quad i \in \left\{ 1, \ldots, N^{\text{batch}} \right\} \tag{2.2}$$

with the dimensionality N^{hidden} of the hidden states, which is a design parameter of the GRU layer. The values of the initial hidden states $\underline{h}_{0,i}$, are typically initialized with zeros or noise [23] but can also be learned by the network, e.g., [5]. The GRU layer processes the time series included in the batch parallely and the data points of the individual time series successively. At the current time step t, the layer's input consists of the batch of the current data points and the fed back batch of previously outputted, hidden states

$$\left(\underline{x}_{t,i}, \ \underline{h}_{t-1,i} \right), \quad i \in \left\{ 1, \ldots, N^{\text{batch}} \right\}. \tag{2.3}$$

For reasons of simplification, the following text only refers to the parallely computed, individual elements of the processed batch. However, the following equations yet explicitly refer to the entire batch.

At every incoming input, the GRU layer at first computes its two gates. The current reset gate

$$\underline{g}_{t,i}^{\text{r}} = \mathcal{F}^{\text{r}} \left(\underline{x}_{t,i}, \underline{h}_{t-1,i} \right), \quad i \in \left\{ 1, \ldots, N^{\text{batch}} \right\} \tag{2.4}$$

is obtained by the mapping

$$\mathcal{F}^{\text{r}} : \left(\mathbb{R}^{N^{\text{in}}}, \ [-1, 1]^{N^{\text{hidden}}} \right) \to [0, 1]^{N^{\text{hidden}}}$$

$$(\underline{x}, \underline{h}) \mapsto \overset{\odot}{\sigma} \left(\underline{\underline{A}}_x^{\text{r}} \underline{x} + \underline{b}_x^{\text{r}} + \underline{\underline{A}}_h^{\text{r}} \underline{h} + \underline{b}_h^{\text{r}} \right). \tag{2.5}$$

---

[3] <code>https://pytorch.org/docs/stable/generated/torch.nn.GRU.html</code>, visited on 09/07/2022

The above mapping to the reset gate can be devided into two steps. First, the current data point and the previous hidden state are linearly transformed with the corresponding matrices of trainable weights and vectors of trainable biases

$$\underline{\underline{A}}_x^{\mathrm{r}} \in \mathbb{R}^{N^{\mathrm{hidden}} \times N^{\mathrm{in}}}, \qquad\qquad \underline{b}_x^{\mathrm{r}} \in \mathbb{R}^{N^{\mathrm{hidden}}},$$
$$\underline{\underline{A}}_h^{\mathrm{r}} \in \mathbb{R}^{N^{\mathrm{hidden}} \times N^{\mathrm{hidden}}}, \qquad\qquad \underline{b}_h^{\mathrm{r}} \in \mathbb{R}^{N^{\mathrm{hidden}}}. \qquad (2.6)$$

The user has the design option to disable all biases of the GRU layer. This is tantamount to set the above and the still upcoming biases of the layer to zero and consider them not trainable. Second, the standard sigmoid function [7] (see figure 2.2)

$$\sigma : \ \mathbb{R} \to [0, 1] \, ; \ x \mapsto \frac{1}{1 + e^{-x}} \qquad (2.7)$$

is applied element-wise (denoted with the accent $\odot$) on the sum of these two linear transformations. The sigmoid function forces the values of the reset gate to be in the interval between zero and one. This is characteristic for a gating mechanism since the gating of a state, which is in fact the calculation of the Hadamard product of the state and the gate, targets at only damping not amplifying or reversing the individual values of the state.

The current update gate

$$\underline{g}_{t,i}^{\mathrm{u}} = \mathcal{F}^{\mathrm{u}} \left(\underline{x}_{t,i}, \underline{h}_{t-1,i} \right), \quad i \in \left\{ 1, \ldots, N^{\mathrm{batch}} \right\} \qquad (2.8)$$

is obtained with the mapping

$$\mathcal{F}^{\mathrm{u}} : \ \left(\mathbb{R}^{N^{\mathrm{in}}}, \ [-1, 1]^{N^{\mathrm{hidden}}} \right) \to [0, 1]^{N^{\mathrm{hidden}}}$$
$$(\underline{x}, \underline{h}) \mapsto \overset{\odot}{\sigma} \left(\underline{\underline{A}}_x^{\mathrm{u}} \underline{x} + \underline{b}_x^{\mathrm{u}} + \underline{\underline{A}}_h^{\mathrm{u}} \underline{h} + \underline{b}_h^{\mathrm{u}} \right). \qquad (2.9)$$

The above mapping to the update gate differs from the mapping to the reset gate only in the fact that the ocurring linear transformations rely on their seperate, trainable weights and biases

$$\underline{\underline{A}}_x^{\mathrm{u}} \in \mathbb{R}^{N^{\mathrm{hidden}} \times N^{\mathrm{in}}}, \qquad\qquad \underline{b}_x^{\mathrm{u}} \in \mathbb{R}^{N^{\mathrm{hidden}}},$$
$$\underline{\underline{A}}_h^{\mathrm{u}} \in \mathbb{R}^{N^{\mathrm{hidden}} \times N^{\mathrm{hidden}}}, \qquad\qquad \underline{b}_h^{\mathrm{u}} \in \mathbb{R}^{N^{\mathrm{hidden}}}. \qquad (2.10)$$

With the knowledge of the current reset gate, the GRU layer calculates the candidate for the current hidden state, hereinafter referred to as candidate state

$$\underline{h}_{t,i}^{\mathrm{c}} = \mathcal{F}^{\mathrm{c}} \left(\underline{x}_{t,i}, \underline{h}_{t-1,i} \right), \quad i \in \left\{ 1, \ldots, N^{\mathrm{batch}} \right\}. \qquad (2.11)$$

The mapping to the candidate state

$$\mathcal{F}^{\mathrm{c}} : \left(\mathbb{R}^{N^{\mathrm{in}}}, [-1, 1]^{N^{\mathrm{hidden}}} \right) \to [-1, 1]^{N^{\mathrm{hidden}}}$$

$$(\underline{x}, \underline{h}) \mapsto \overset{\odot}{\tanh} \left[\underline{\underline{A}}_x^{\mathrm{c}} \underline{x} + \underline{b}_x^{\mathrm{c}} + \mathcal{F}^{\mathrm{r}}(\underline{x}, \underline{h}) \odot \left(\underline{\underline{A}}_h^{\mathrm{c}} \underline{h} + \underline{b}_h^{\mathrm{c}} \right) \right] \qquad (2.12)$$

contains the trainable weight matrices and bias vectors

$$\underline{\underline{A}}_x^{\mathrm{c}} \in \mathbb{R}^{N^{\mathrm{hidden}} \times N^{\mathrm{in}}}, \qquad\qquad \underline{b}_x^{\mathrm{c}} \in \mathbb{R}^{N^{\mathrm{hidden}}},$$

$$\underline{\underline{A}}_h^{\mathrm{c}} \in \mathbb{R}^{N^{\mathrm{hidden}} \times N^{\mathrm{hidden}}}, \qquad\qquad \underline{b}_h^{\mathrm{c}} \in \mathbb{R}^{N^{\mathrm{hidden}}}. \qquad (2.13)$$

The above mapping to the candidate state resembles the mappings to the reset and update gate by subjecting the current data point and the previous hidden state to a seperate, biased linear transformation. It differs in two aspects. First, before the two transformations are added together, the current reset gate is applied on the transformed, previous hidden state ($\odot$ denotes the Hadamard product). The function of the reset gate is, consequently, to mitigate the contribution of the previous hidden state to the candidate state. Second, instead of the sigmoid function, the hyperbolic tangent [20] (see figure 2.2)

$$\tanh : \ \mathbb{R} \to [-1, 1] \,; \ x \mapsto \frac{e^x - e^{-x}}{e^x + e^{-x}} \qquad (2.14)$$

is applied element-wise on the sum of the linearly transformed data point and the gated, linearly transformed, previous hidden state. The hyperbolic tangent bounds the values of the candidate state to the interval from minus to plus one.

Finally, the GRU layer computes the current hidden state

$$h_{t,i} = \mathcal{F}^{\mathrm{h}} \left(\underline{x}_{t,i}, \underline{h}_{t-1,i} \right), \quad i \in \left\{ 1, \dots, N^{\mathrm{batch}} \right\} \qquad (2.15)$$

on the basis of the mapping

$$\mathcal{F}^{\mathrm{h}} : \left(\mathbb{R}^{N^{\mathrm{in}}}, \ [-1, 1]^{N^{\mathrm{hidden}}} \right) \to [-1, 1]^{N^{\mathrm{hidden}}}$$

$$\chi := (\underline{x}, \ \underline{h}) \mapsto [\underline{1} - \mathcal{F}^{\mathrm{u}}(\chi)] \odot \mathcal{F}^{\mathrm{c}}(\chi) + \mathcal{F}^{\mathrm{u}}(\chi) \odot \underline{h}. \qquad (2.16)$$

The above mapping to the hidden state is basically a weighted arithmetic mean. Before the previous hidden state and the current candidate state are averaged, they are weighted by the current update gate and counter-update gate, respectively. In other words, the update gate, whose values are between zero and one, controls the element-wise percentage proportions of both states on the current hidden state. Due to the fact that the hyperbolic tangent normalizes the elements of the candidate state to the interval from minus to plus one (equation 2.12) and the values of the initial hidden state are typically initialized to be also within this interval (equation 2.2), the values of the current hidden state are also bounded to the interval from minus to plus one.
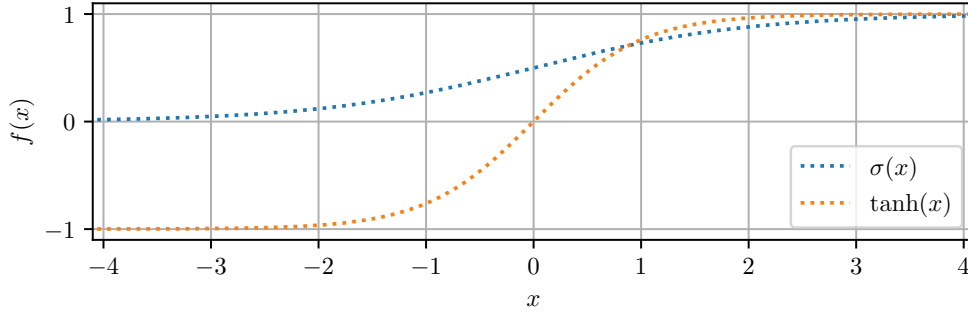
Figure 2.2: The non-linear activation functions deployed within a standard GRU. The standard sigmoid function $\sigma(x) = (1 + e^{-x})^{-1}$ normalizes the values of the reset and update gate to the interval from zero to one (equation 3.27 and 2.9). The hyperbolic tangent $\tanh(x) = (e^x - e^{-x})(e^x + e^{-x})^{-1}$ normalizes the values of the candidate and, consequently, the hidden state to the interval from minus to plus one (equation 2.12 and 2.16).

Backpropagation through time

The following presents the application of backpropagation through time on a single integrated GRU layer operating in many-to-one mode in order to calculate the gradients of the loss with respect to the GRU layer's trainable parameters. During training, these gradients are required by gradient-based methods which update the trainable parameters with the target to minimize the loss.

Let a single GRU layer, integrated into any superior ANN, operate in many-to-one mode. With biases enabled, the set of all structures that contain trainable parameters of the GRU layer is aggregated from equation 2.6, 2.10 and 2.13

$$\Theta = \left\{ \underline{\underline{A}}^{\mathrm{r}}_x, \underline{b}^{\mathrm{r}}_x, \underline{\underline{A}}^{\mathrm{r}}_h, \underline{b}^{\mathrm{r}}_h, \underline{\underline{A}}^{\mathrm{u}}_x, \underline{b}^{\mathrm{u}}_x, \underline{\underline{A}}^{\mathrm{u}}_h, \underline{b}^{\mathrm{u}}_h, \underline{\underline{A}}^{\mathrm{c}}_x, \underline{b}^{\mathrm{c}}_x, \underline{\underline{A}}^{\mathrm{c}}_h, \underline{b}^{\mathrm{c}}_h \right\}. \tag{2.17}$$

The addition of the sizes of the structurs in the set Θ yields the total number of trainable parameters of the GRU layer

$$N^{\mathrm{param}} = \begin{cases} 3N^{\mathrm{hidden}} \left(N^{\mathrm{in}} + N^{\mathrm{hidden}} + 2 \right), & \text{if biases enabled} \\ 3N^{\mathrm{hidden}} \left(N^{\mathrm{in}} + N^{\mathrm{hidden}} \right), & \text{else.} \end{cases} \tag{2.18}$$

At a single inference, the GRU layer receives a batch of sequences of feature vectors from the previous layer of the ANN

$$(\underline{x}_t)_{t \in \{1,\dots,N^{\mathrm{seq}}\},i}, \quad i \in \left\{ 1, \dots, N^{\mathrm{batch}} \right\}. \tag{2.19}$$

The GRU layer in many-to-one mode maps each incoming batch of sequences to a batch of single outputs, whereby a single output is the hidden state lastly infered from a
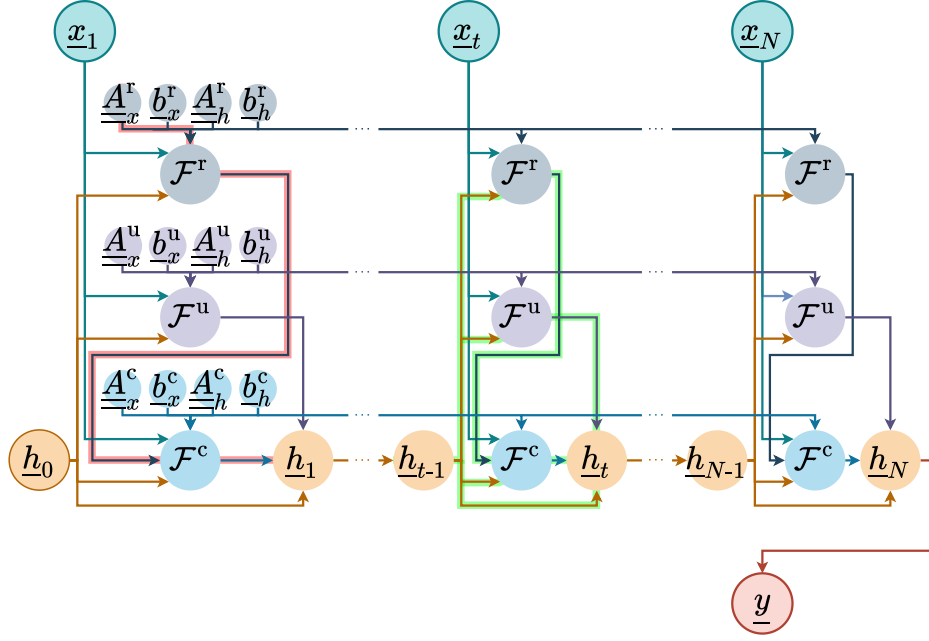
Figure 2.3: Time-unfolded computation graph of a GRU layer operating in many-to-one mode. The input sequence $(x_t)_{t \in \{1, \dots N\}}$ is mapped to the single output $\underline{y}$ which is equal to the lastly inferred, hidden state $\underline{h}_N$. Equation 3.27, 2.9 and 2.12 define the mapping to the reset gate $\mathcal{F}^r$, update gate $\mathcal{F}^u$ and candidate state $\mathcal{F}^c$, respectively. The hidden states $(h_t)_{t \in \{1, \dots N\}}$ are obtained with the mapping $\mathcal{F}^h$ defined by equation 2.16 whereas the initial hidden state $\underline{h}_0$ (equation 2.2) is defined by the user. The trainable parameters $\underline{\underline{A}}^{\square}_{\square}, \underline{b}^{\square}_{\square}$ of the GRU layer are shared across all unfolded time steps. The backpropagation path of the intra-gradient with respect to $\underline{\underline{A}}^r_x$ (equation 2.24) is highlighted in red for the first time step $t = 1$. The backpropagation paths of the inter-gradient (equation 2.27) is highlighted in green for the time step t.

sequence

$$\underline{y}_i = \underline{h}_{N^{seq},i}, \quad i \in \left\{ 1, \dots, N^{\text{batch}} \right\}. \tag{2.20}$$

The time-unfolded computation graph of the integrated GRU layer for a single batch element is shown in figure 2.3. The batches of single GRU outputs are forwarded to the subsequent layer of the ANN. Whenever a batch has passed all the output layer of the ANN, the loss L of the batch is computed by averaging the losses of the individual elements of the batch. Because the seperate losses depend on their corresponding single GRU output, the loss of the batch is a function of all of these outputs.

$$L \left(\underline{y}_1, \dots, \underline{y}_{N^{\text{batch}}} \right) = \frac{1}{N^{\text{batch}}} \sum_{i=1}^{N^{\text{batch}}} L_i \left(\underline{y}_i \right). \tag{2.21}$$

11

Gradient-based methods update the trainable parameters of the ANN with the goal to minimize the loss of the batch. For this, they require the knwoledge of the gradients of the loss with respect to the trainable parameters. The update of the trainable parameters of the integrated GRU layer complies with

$$\underset{\Theta}{\mathrm{argmin}}\, L\left(\underline{y}_1,\ldots,\underline{y}_{N^{\text{batch}}}\right).\tag{2.22}$$

In conformity with Li [15], the gradient of the batch loss with respect to a single element $\theta \in \Theta$ of the set of structures containing trainable parameters (equation 2.17) is computed based on backpropagation through time

$$
\begin{aligned}
&\frac{\partial}{\partial\theta} L\left(\underline{y}_1,\ldots,\underline{y}_{N^{\text{batch}}}\right)\\
&\overset{(1)}{=} \frac{1}{N^{\text{batch}}}\sum_{i=1}^{N^{\text{batch}}} \frac{\partial}{\partial\theta} L_i\left(\underline{y}_i\right)\\
&\overset{(2)}{=} \frac{1}{N^{\text{batch}}}\sum_{i=1}^{N^{\text{batch}}} \left(\frac{\partial L_i}{\partial\underline{y}_i}\frac{\partial\underline{y}_i}{\partial\theta}\right)\\
&\overset{(3)}{=} \frac{1}{N^{\text{batch}}}\sum_{i=1}^{N^{\text{batch}}} \left[\frac{\partial L_i}{\partial\underline{y}_i}\sum_{j=1}^{N^{seq}}\left(\frac{\partial\underline{y}_i}{\partial\underline{h}_{j,i}}\frac{\widehat{\partial\underline{h}_{j,i}}}{\partial\theta}\right)\right]\\
&\overset{(4)}{=} \frac{1}{N^{\text{batch}}}\sum_{i=1}^{N^{\text{batch}}} \left\{\frac{\partial L_i}{\partial\underline{y}_i}\sum_{j=1}^{N^{seq}}\left[\prod_{k=j+1}^{N^{seq}}\left(\frac{\partial\underline{h}_{k,i}}{\partial\underline{h}_{k-1,i}}\right)\frac{\widehat{\partial\underline{h}_{j,i}}}{\partial\theta}\right]\right\}.
\end{aligned}\tag{2.23}
$$

(1) Loss of a batch (equ. 2.21)

(2) Chain rule

(3) Backpropagation through time (gradient $\widehat{\square}$ considers previous hidden states constant)

(4) Many-to-one output (equ. 2.20); chain rule applied on $\partial\underline{y}_i/\partial\underline{h}_{j,i}$

In the above formula, the gradient $\widehat{\partial\underline{h}_{j,i}/\partial\theta}$, hereinafter referred to as intra-gradient, treats all previous hidden states $\underline{h}_{\tilde{j},\ldots,i}$, $\tilde{j}\in\{0,j-1\}$ as constants. In doing so, the intra-gradient only covers the backpropagation path from the hidden state $\underline{h}_{j,i}$ to the parameter structure θ within the same time step j. In order to compute the full gradient covering all backpropagation paths to θ, all intra-backpropagation paths are connected through time to the GRU layer's output $\underline{y}_i$ by multiplying the intra-gradients with their corresponding chain of time step inter-gradients $\partial\underline{h}_{k,i}/\partial\underline{h}_{k-1,i}$. For demonstration purposes, the intra-gradient with respect to $\theta = \underline{\underline{A}}^{\mathrm{r}}_x$ (the corresponding backpropagation path is highlighted

for the first time step in figure 2.3) is examplarily derived as

$$
\begin{aligned}
\frac{\partial \widehat{\underline{h}_{t,i}}}{\partial \underline{\underline{A}}^{\mathrm{r}}_x} &\overset{(1)}{=} \frac{\widehat{\partial}}{\partial \underline{\underline{A}}^{\mathrm{r}}_x} \left\{ [\underline{1} - \mathcal{F}^{\mathrm{u}}(\chi)] \odot \mathcal{F}^{\mathrm{c}}(\chi) + \mathcal{F}^{\mathrm{u}}(\chi) \odot \underline{h}_{t\text{-}1,i} \right\} \\
&\overset{(2)}{=} \operatorname{diag}\left[\underline{1} - \mathcal{F}^{\mathrm{u}}(\chi)\right] \frac{\partial \widehat{\mathcal{F}^{\mathrm{c}}(\chi)}}{\partial \underline{\underline{A}}^{\mathrm{r}}_x}
\end{aligned} \tag{2.24}
$$

(1) Mapping to hidden state (equ. 2.15, 2.16); $\chi := \left(\underline{x}_{t,i}, \underline{h}_{t\text{-}1,i}\right)$

(2) Sum rule of differentiation;

Mapping to update gate (equ. 2.9): $\partial \widehat{\mathcal{F}^{\mathrm{u}}} / \partial \underline{\underline{A}}^{\mathrm{r}}_x = 0$

Consider previous hidden states constant: $\partial \widehat{\underline{h}_{t\text{-}1,i}} / \partial \underline{\underline{A}}^{\mathrm{r}}_x = 0$;

Hadamard product of two vectors (equ. 2.33)

with

$$
\begin{aligned}
\frac{\partial \widehat{\mathcal{F}^{\mathrm{c}}(\chi)}}{\partial \underline{\underline{A}}^{\mathrm{r}}_x} &\overset{(1)}{=} \frac{\widehat{\partial}}{\partial \underline{\underline{A}}^{\mathrm{r}}_x} \left\{ \overset{\odot}{\tanh} \left[\underbrace{ \underline{\underline{A}}^{\mathrm{c}}_x \underline{x}_{t,i} + \underline{b}^{\mathrm{c}}_x + \mathcal{F}^{\mathrm{r}}\left(\underline{x}_{t,i}, \underline{h}_{t\text{-}1,i}\right) \odot \left(\underline{\underline{A}}^{\mathrm{c}}_h \underline{h}_{t\text{-}1,i} + \underline{b}^{\mathrm{c}}_h \right) }_{:=\chi^{\mathrm{c}}} \right] \right\} \\
&\overset{(2)}{=} \operatorname{diag}\left[\frac{\partial}{\partial \chi^{\mathrm{c}}} \overset{\odot}{\tanh}(\chi^{\mathrm{c}}) \right] \cdot \frac{\partial \widehat{\chi^{\mathrm{c}}}}{\partial \underline{\underline{A}}^{\mathrm{r}}_x} \\
&\overset{(3)}{=} \operatorname{diag}\left[1 - \overset{\odot}{\tanh}^2(\chi^{\mathrm{c}}) \right] \cdot \operatorname{diag}\left(\underline{\underline{A}}^{\mathrm{c}}_h \underline{h}_{t-1,i} + \underline{b}^{\mathrm{c}}_h \right) \frac{\partial \mathcal{F}^{\mathrm{r}} \widehat{\left(\underline{x}_{t,i}, \underline{h}_{t\text{-}1,i}\right)}}{\partial \underline{\underline{A}}^{\mathrm{r}}_x}
\end{aligned} \tag{2.25}
$$

(1) Mapping to candidate state (equ. 2.12); $\chi := \left(\underline{x}_{t,i}, \underline{h}_{t\text{-}1,i}\right)$

(2) Chain rule of differentiation;

Derivative of function applied element-wise on vector (equ. 2.35)

(3) Derivative of hyperbolic tangent (equ. 2.31);

Hadamard product of two vectors (equ. 2.33)

and

$$\frac{\partial \mathcal{F}^{\mathrm{r}} \overbrace{(\underline{x}_{t,i}, \underline{h}_{t\text{-}1,i})}}{\partial \underline{\underline{A}}^{\mathrm{r}}_x} \overset{(1)}{=} \frac{\widehat{\partial}}{\partial \underline{\underline{A}}^{\mathrm{r}}_x} \left[\overset{\odot}{\sigma} \left(\underbrace{\underline{\underline{A}}^{\mathrm{r}}_x \underline{x}_{t,i} + \underline{b}^{\mathrm{r}}_x + \underline{\underline{A}}^{\mathrm{r}}_h \underline{h}_{t\text{-}1,i} + \underline{b}^{\mathrm{r}}_h}_{:=\chi^{\mathrm{r}}} \right) \right]$$

$$\overset{(2)}{=} \mathrm{diag} \left[\frac{\partial}{\partial \chi^{\mathrm{r}}} \overset{\odot}{\sigma} (\chi^{\mathrm{r}}) \right] \cdot \frac{\widehat{\partial \chi^{\mathrm{u}}}}{\partial \underline{\underline{A}}^{\mathrm{r}}_x}$$

$$\overset{(3)}{=} \mathrm{diag} \left\{ \overset{\odot}{\sigma} (\chi^{\mathrm{r}}) \odot \left[\underline{1} - \overset{\odot}{\sigma} (\chi^{\mathrm{r}}) \right] \right\} \cdot \frac{\partial \underline{\underline{A}}^{\mathrm{r}}_x \underline{x}_{t,i}}{\partial \underline{\underline{A}}^{\mathrm{r}}_x}. \tag{2.26}$$

For the computation of the gradient $\partial \left(\underline{\underline{A}}^{\mathrm{r}}_x \underline{x}_{t,i} \right) / \partial \underline{\underline{A}}^{\mathrm{r}}_x$, which is a 3-dimensional matrix whose information content is only 2-dimensional, refer to [14], for example.

The in equation 2.23 required inter-gradient (the corresponding backpropagation path is highlighted in figure 2.3) , i.e., the gradient of the current hidden state with respect to the previous hidden state, is derived as

$$\frac{\partial \underline{h}_{t,i}}{\partial \underline{h}_{t\text{-}1,i}} \overset{(1)}{=} \frac{\partial}{\partial \underline{h}_{t\text{-}1,i}} \left\{ [\underline{1} - \mathcal{F}^{\mathrm{u}} (\chi)] \odot \mathcal{F}^{\mathrm{c}} (\chi) + \mathcal{F}^{\mathrm{u}} (\chi) \odot \underline{h}_{t-1,i} \right\}$$

$$\overset{(2)}{=} \frac{\partial}{\partial \underline{h}_{t\text{-}1,i}} \left\{ [\underline{1} - \mathcal{F}^{\mathrm{u}} (\chi)] \odot \mathcal{F}^{\mathrm{c}} (\chi) \right\} + \frac{\partial}{\partial \underline{h}_{t\text{-}1,i}} \left\{ \mathcal{F}^{\mathrm{u}} (\chi) \odot \underline{h}_{t-1,i} \right\}$$

$$\overset{(3)}{=} -\mathrm{diag} \left[\mathcal{F}^{\mathrm{c}} (\chi) \right] \frac{\partial \mathcal{F}^{\mathrm{u}} (\chi)}{\partial \underline{h}_{t\text{-}1,i}} + \mathrm{diag} \left[\underline{1} - \mathcal{F}^{\mathrm{u}} (\chi) \right] \frac{\partial \mathcal{F}^{\mathrm{c}} (\chi)}{\partial \underline{h}_{t\text{-}1,i}}$$

$$+ \mathrm{diag} \left(\underline{h}_{t-1,i} \right) \frac{\partial \mathcal{F}^{\mathrm{u}} (\chi)}{\partial \underline{h}_{t\text{-}1,i}} + \mathrm{diag} \left[\mathcal{F}^{\mathrm{u}} (\chi) \right]. \tag{2.27}$$

The in equation 2.27 required gradient of the current update gate with respect to the

previous hidden state is derived as

$$
\frac{\partial \mathcal{F}^{\mathrm{u}}\left(\underline{x}_{t,i}, \underline{h}_{t\text{-}1,i}\right)}{\partial \underline{h}_{t\text{-}1,i}} \overset{(1)}{=} \frac{\partial}{\partial \underline{h}_{t\text{-}1,i}} \left[\overset{\odot}{\sigma} \left(\underbrace{\underline{\underline{A}}^{\mathrm{u}}_x \underline{x}_{t,i} + \underline{b}^{\mathrm{u}}_x + \underline{\underline{A}}^{\mathrm{u}}_h \underline{h}_{t\text{-}1,i} + \underline{b}^{\mathrm{u}}_h}_{:=\chi^{\mathrm{u}}} \right) \right]
$$

$$
\overset{(2)}{=} \mathrm{diag}\left[\frac{\partial}{\partial \chi^{\mathrm{u}}} \overset{\odot}{\sigma}\left(\chi^{\mathrm{u}}\right) \right] \cdot \frac{\partial}{\partial \underline{h}_{t\text{-}1,i}} \chi^{\mathrm{u}}
$$

$$
\overset{(3)}{=} \mathrm{diag}\left\{ \overset{\odot}{\sigma}\left(\chi^{\mathrm{u}}\right) \odot \left[1 - \overset{\odot}{\sigma}\left(\chi^{\mathrm{u}}\right) \right] \right\} \cdot \underline{\underline{A}}^{\mathrm{u}}_h. \tag{2.28}
$$

The in equation 2.27 required gradient of the current candidate state with respect to the previous hidden state is derived as

$$
\frac{\partial}{\partial \underline{h}_{t\text{-}1,i}} \mathcal{F}^{\mathrm{c}}\left(\underline{x}_{t,i}, \underline{h}_{t\text{-}1,i}\right)
$$

$$
\overset{(1)}{=} \frac{\partial}{\partial \underline{h}_{t\text{-}1,i}} \left\{ \overset{\odot}{\tanh} \left[\underbrace{\underline{\underline{A}}^{\mathrm{c}}_x \underline{x}_{t,i} + \underline{b}^{\mathrm{c}}_x + \mathcal{F}^{\mathrm{r}}\left(\underline{x}_{t,i}, \underline{h}_{t\text{-}1,i}\right) \odot \left(\underline{\underline{A}}^{\mathrm{c}}_h \underline{h}_{t\text{-}1,i} + \underline{b}^{\mathrm{c}}_h \right)}_{:=\chi^{\mathrm{c}}} \right] \right\}
$$

$$
\overset{(2)}{=} \mathrm{diag}\left[\frac{\partial}{\partial \chi^{\mathrm{c}}} \overset{\odot}{\tanh}\left(\chi^{\mathrm{c}}\right) \right] \cdot \frac{\partial}{\partial \underline{h}_{t\text{-}1,i}} \chi^{\mathrm{c}}
$$

$$
\overset{(3)}{=} \mathrm{diag}\left[1 - \overset{\odot}{\tanh}{}^2\left(\chi^{\mathrm{c}}\right) \right]
$$

$$
\cdot \left\{ \mathrm{diag}\left(\underline{\underline{A}}^{\mathrm{c}}_h \underline{h}_{t-1,i} + \underline{b}^{\mathrm{c}}_h \right) \frac{\partial \mathcal{F}^{\mathrm{r}}\left(\underline{x}_{t,i}, \underline{h}_{t\text{-}1,i}\right)}{\partial \underline{h}_{t\text{-}1,i}} + \mathrm{diag}\left[\mathcal{F}^{\mathrm{r}}\left(\underline{x}_{t,i}, \underline{h}_{t\text{-}1,i}\right) \right] \underline{\underline{A}}^{\mathrm{c}}_h \right\}. \tag{2.29}
$$

The in equation 2.29 required gradient of the current reset gate with respect to the previous hidden state shares the same structure with the gradient of equation 2.28 and is

hence derived as

$$\frac{\partial}{\partial \underline{h}_{t\text{-}1,i}} \mathcal{F}^{\mathrm{r}}\left(\underline{x}_{t,i}, \underline{h}_{t\text{-}1,i}\right) = \mathrm{diag}\left\{\overset{\odot}{\sigma}\left(\underline{\chi}^{\mathrm{r}}\right) \odot \left[1 - \overset{\odot}{\sigma}\left(\underline{\chi}^{\mathrm{r}}\right)\right]\right\} \cdot \underline{\underline{A}}^{\mathrm{r}}_{h}$$

$$\text{with } \underline{\chi}^{\mathrm{r}} := \underline{\underline{A}}^{\mathrm{r}}_x \underline{x}_{t,i} + \underline{b}^{\mathrm{r}}_x + \underline{\underline{A}}^{\mathrm{r}}_h \underline{h}_{t\text{-}1,i} + \underline{b}^{\mathrm{r}}_h. \tag{2.30}$$

The above derivations revert to the following equations. Equations (4.5.73) and (4.5.17) of Abramowitz and Stegun [20] yield the derivative of the hyperbolic tangent as

$$\frac{\mathrm{d}}{\mathrm{d}x} \tanh(x) = 1 - \tanh^2(x). \tag{2.31}$$

The derivative of the sigmoid function (e.g., [16]) is given by

$$\frac{\mathrm{d}}{\mathrm{d}x} \sigma\left(x\right) = \sigma\left(x\right)\left[1 - \sigma\left(x\right)\right]. \tag{2.32}$$

The hadamard product of two vectors can be reformulated as the matrix product of a diagonal matrix and a vector [2]

$$\underline{x}_1 \odot \underline{x}_2 = \mathrm{diag}\left(\underline{x}_1\right)\underline{x}_2 = \mathrm{diag}\left(\underline{x}_2\right)\underline{x}_1. \tag{2.33}$$

Together with the product rule of differentiation, the derivative of the Hadamard product of two vectors is therewith identified as

$$\frac{\partial}{\partial t}\left(\underline{x}_1 \odot \underline{x}_2\right) = \mathrm{diag}\left(\underline{x}_2\right)\frac{\partial \underline{x}_1}{\partial t} + \mathrm{diag}\left(\underline{x}_1\right)\frac{\partial \underline{x}_2}{\partial t}. \tag{2.34}$$

The derivative of a function $f : \mathbb{R} \to \mathbb{R}$, that is applied element-wise on a vector $\underline{x}$, is the diagonal matrix built from the derivative of the function applied element-wise on the vector

$$\frac{\partial}{\partial \underline{x}} \overset{\odot}{f}\left(\underline{x}\right) = \mathrm{diag}\left[\overset{\odot}{f'}\left(\underline{x}\right)\right]. \tag{2.35}$$

The above statement can be derived from the calculation of the differential of the function

$$\frac{\mathrm{d}}{\mathrm{d}\underline{x}} \overset{\odot}{f}\left(\underline{x}\right) \cdot \mathrm{d}\underline{x} \overset{(1)}{=} \mathrm{d}\overset{\odot}{f}\left(\underline{x}\right) \overset{(2)}{=} \left[\overset{\odot}{f'}\left(\underline{x}\right)\right] \odot \mathrm{d}\underline{x} \overset{(3)}{=} \mathrm{diag}\left[\overset{\odot}{f'}\left(\underline{x}\right)\right] \cdot \mathrm{d}\underline{x}. \tag{2.36}$$

(1) Relation of differential and derivative

(2) Chain rule element-wise applied

(3) Hadamard product of two vectors (equ. 2.33) $\tag{2.37}$

Chapter 3

Navigation Method

DELETEME: In this chapter you start addressing your actual problem. Therefore, it makes often sense to make a detailed problem analysis first (if not done in introduction). You should be sure about what to do and how. As writtin in the background part, it might also make sense to include complex background information or papers you are basing on in this analysis. If you are solving a software problem, you should follow the state of the art of software development which basically includes: problem analysis, design, implementation, testing, and deployment. Maintenance is often also described but I believe this will not be required for most theses. Code should be placed in the appendix unless it is solving an essential aspect of your work.

In order to investigate the effect of temporal comprehension in machine-learning-based, autonomous navigation of drones, this master thesis extends the navigation method of Kaufmann, Loquercio et. al [?] is minimally adjusted and extended with a recurrent convolutional neural network. This chapter ...

3.1 Reference systems

In this thesis, a point $\underline{p}$ relates to either the global, the local or the image reference system

$$\mathbf{G}\underline{p} = \begin{bmatrix} \mathbf{G}x \\ \mathbf{G}y \\ \mathbf{G}z \end{bmatrix} \in \mathbb{R}^3, \quad \mathbf{L}\underline{p} = \begin{bmatrix} \mathbf{L}x \\ \mathbf{L}y \\ \mathbf{L}z \end{bmatrix} \in \mathbb{R}^3, \quad \mathbf{I}\underline{p} = \begin{bmatrix} \mathbf{I}x \\ \mathbf{I}y \end{bmatrix} \in \mathbb{R}^2_{[-1,1]}. \tag{3.1}$$

The global reference system is fixed to an arbitrary point on the earth and hence quasi inertial. It is spanned by the orthonormal basis which, related to the global system, equates to the standard basis of $\mathbb{R}^3$

$$\left\{ \underline{e}_x^{\mathbf{G}}, \underline{e}_y^{\mathbf{G}}, \underline{e}_z^{\mathbf{G}} \right\} \quad \text{with} \quad \mathbf{G}\underline{e}_x^{\mathbf{G}} = \begin{bmatrix} 1 \\ 0 \\ 0 \end{bmatrix}, \ \mathbf{G}\underline{e}_y^{\mathbf{G}} = \begin{bmatrix} 0 \\ 1 \\ 0 \end{bmatrix}, \ \mathbf{G}\underline{e}_z^{\mathbf{G}} = \begin{bmatrix} 0 \\ 0 \\ 1 \end{bmatrix}. \tag{3.2}$$

The local reference system (see figure 3.1a) is fixed to the moving drone. Its orthonormal basis

$$\left\{\underline{e}_x^{\mathrm{L}}, \underline{e}_y^{\mathrm{L}}, \underline{e}_z^{\mathrm{L}}\right\} \quad \text{with} \quad {}_{\mathrm{L}}\underline{e}_x^{\mathrm{L}} = \begin{bmatrix} 1 \\ 0 \\ 0 \end{bmatrix}, \; {}_{\mathrm{L}}\underline{e}_y^{\mathrm{L}} = \begin{bmatrix} 0 \\ 1 \\ 0 \end{bmatrix}, \; {}_{\mathrm{L}}\underline{e}_z^{\mathrm{L}} = \begin{bmatrix} 0 \\ 0 \\ 1 \end{bmatrix} \tag{3.3}$$

origins at the optical center of the onboard camera. The unit vector $\underline{e}_x^{\mathrm{L}}$ points along the optical axis of the camera in the flight direction of the drone. The unit vector $\underline{e}_z^{\mathrm{L}}$ points in the direction of the forces generated by the rotors and is parallel to the vertical axis of the image plane of the camera. The unit vector $\underline{e}_y^{\mathrm{L}}$ points to the left of the drone paralleling the horizontal axis of the image plane.

The image reference system (see figure 3.1b) is superimposed on the images of the onboard camera. This 2-dimensional system is spanned by the orthonormal basis

$$\left\{\underline{e}_x^{\mathrm{I}}, \underline{e}_y^{\mathrm{I}}\right\} \; \text{with} \; {}_{\mathrm{I}}\underline{e}_x^{\mathrm{I}} = \begin{bmatrix} 1 \\ 0 \end{bmatrix}, \; {}_{\mathrm{I}}\underline{e}_y^{\mathrm{I}} = \begin{bmatrix} 0 \\ 1 \end{bmatrix}. \tag{3.4}$$

The origin of the image reference system is located at the center of the image plane. The unit vector $\underline{e}_x^{\mathrm{I}}$ points rightwards along the vertical axis of the image plane. The unit vector $\underline{e}_y^{\mathrm{I}}$ points upwards along the horizontal axis of the image plane. A point on the image plane is bounded by the left and right $-1 \leq {}_{\mathrm{I}}x \leq 1$ as well as the lower and upper $-1 \leq {}_{\mathrm{I}}y \leq 1$ border of the image plane.

The global reference system is only referred to by the expert system (see section) which makes navigation decisions based on globally consistent information when generating training data for the ANN module. The autonomous navigation method, with the fully trained ANN module making the navigation decisions, exclusively resorts to data from onboard sensors, which is relative to the drone and its onboard camera. The method, therefore, operates only within the local and image reference system.

Transformation between the global and the local reference system

The drone position ${}_{\mathrm{G}}\underline{p}^{\mathrm{drone}}$ and quaternion orientation ${}_{\mathrm{G}}\underline{q}^{\mathrm{drone}}$ in the global reference system fully determine the the transformation from the global to the local reference system and vice versa. The bijective transformation of a point from the global to the local reference system is given by

$$T_{\mathbf{LG}} : \mathbb{R}^3 \to \mathbb{R}^3$$

$${}_{\mathrm{G}}\underline{p} = \begin{bmatrix} {}_{\mathbf{G}}x \\ {}_{\mathbf{G}}y \\ {}_{\mathbf{G}}z \end{bmatrix} \mapsto {}_{\mathrm{L}}\underline{p} = \begin{bmatrix} {}_{\mathbf{L}}x \\ {}_{\mathbf{L}}y \\ {}_{\mathbf{L}}z \end{bmatrix} = \mathcal{P}\left[\mathrm{inv}\left({}_{\mathbf{G}}\underline{q}^{\mathrm{drone}}\right) * \mathcal{Q}\left({}_{\mathbf{G}}\underline{p} - {}_{\mathbf{G}}\underline{p}^{\mathrm{drone}}\right) * {}_{\mathbf{G}}\underline{q}^{\mathrm{drone}}\right]. \tag{3.5}$$

(a) Local reference system
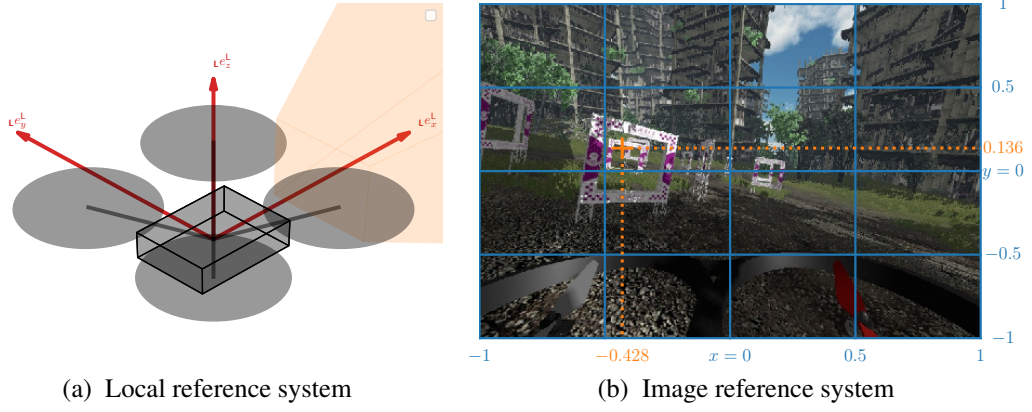

(b) Image reference system

Figure 3.1: The local and the image reference system. The former is aligned with the drone and its onboard camera while the latter is superimposed on the images of the onboard camera. For the image reference system, the waypoint $_{\mathbf{I}}\underline{p}^{\text{wayp}} = \begin{bmatrix} -0.428 & 0.136 \end{bmatrix}^T$ (orange) , that belongs to the same training data sample as the underlying image, is depicted.

The inverse transformation from the local to the global reference system is given by

$$T_{\mathbf{GL}} : \mathbb{R}^3 \to \mathbb{R}^3$$

$$_{\mathbf{L}}\underline{p} = \begin{bmatrix} _{\mathbf{L}}x \\ _{\mathbf{L}}y \\ _{\mathbf{L}}z \end{bmatrix} \mapsto {_{\mathbf{G}}}\underline{p} = \begin{bmatrix} _{\mathbf{G}}x \\ _{\mathbf{G}}y \\ _{\mathbf{G}}z \end{bmatrix} = \mathcal{P} \left[{_{\mathbf{G}}}\underline{q}^{\text{drone}} * \mathcal{Q}\left({_{\mathbf{G}}}\underline{p}\right) * \text{inv}\left({_{\mathbf{G}}}\underline{q}^{\text{drone}}\right) \right] + {_{\mathbf{G}}}\underline{p}^{\text{drone}}.$$

(3.6)

In the above transformations, $\mathcal{Q}$ and $\mathcal{P}$ map points to their quaternion representations and vice versa

$$\mathcal{Q} : \mathbb{R}^3 \to \mathbb{R}^4; \ \underline{p} = \begin{bmatrix} x \\ y \\ z \end{bmatrix} \mapsto \underline{q} = \begin{bmatrix} w \\ \underline{p} \end{bmatrix} \text{ with } w = 0$$

$$\mathcal{P} : \mathbb{R}^4 \to \mathbb{R}^3; \ \underline{q} = \begin{bmatrix} w \\ \underline{p} \end{bmatrix} \mapsto \underline{p} = \begin{bmatrix} x \\ y \\ z \end{bmatrix},$$

(3.7)

the operator $*$ denotes the quaternion multiplication

$$\underline{q}_0 * \underline{q}_1 = \begin{bmatrix} w_0 w_1 - \underline{p}_0^T \underline{p}_1 \\ w_0 \underline{p}_1 + w_1 \underline{p}_0 + \underline{p}_0 \times \underline{p}_1 \end{bmatrix}$$

(3.8)

19

and the inversion of a quaternion is given by

$$\text{inv}(\underline{q}) = \frac{1}{\|\underline{q}\|_2} \begin{bmatrix} w \\ -\underline{p} \end{bmatrix}. \tag{3.9}$$

Both transformations are the inversion of each other, i.e., points are transformed without forfeiting information

$$T_{\mathbf{GL}} \circ T_{\mathbf{LG}} \left({}_{\mathbf{G}}p \right) = {}_{\mathbf{G}}p, \quad T_{\mathbf{LG}} \circ T_{\mathbf{GL}} \left({}_{\mathbf{L}}p \right) = {}_{\mathbf{L}}p. \tag{3.10}$$

Transformation between the local and the image reference system

The horizontal $\phi_{z,\text{camera}}^{\text{user}}$ and the vertical $\phi_{y,\text{camera}}^{\text{user}}$ angle of view of the onboard camera, both specified by the user, fully determine the transformation of a point from the local to the image reference system

$$T_{\mathbf{IL}} : \mathbb{R}^3 \to \mathbb{R}^2_{[-1,1]}$$

$$\mathbf{L}\underline{p} = \begin{bmatrix} \mathbf{L}x \\ \mathbf{L}y \\ \mathbf{L}z \end{bmatrix} \mapsto \mathbf{I}\underline{p} = \begin{bmatrix} \mathbf{I}x \\ \mathbf{I}y \end{bmatrix} = \begin{bmatrix} \max\left\{-1, \min\left\{-\frac{1}{\frac{1}{2}\phi_{z,\text{camera}}^{\text{user}}}\text{atan2}\left({}_{\mathbf{L}}y, {}_{\mathbf{L}}x\right), 1\right\}\right\} \\ \max\left\{-1, \min\left\{\frac{1}{\frac{1}{2}\phi_{y,\text{camera}}^{\text{user}}}\text{atan2}\left({}_{\mathbf{L}}z, \|{}_{\mathbf{L}}\underline{p}\|_2\right), 1\right\}\right\} \end{bmatrix}. \tag{3.11}$$

The above transformation can be interpreted as a projection of a point onto the image plane obtained by normalizing the yaw $\text{atan2}\left({}_{\mathbf{L}}y, {}_{\mathbf{L}}x\right)$ and pitch $\text{atan2}\left({}_{\mathbf{L}}z, \|{}_{\mathbf{L}}\underline{p}\|_2\right)$ angle of the vector from ${}_{\mathbf{L}}\underline{0}$ to ${}_{\mathbf{L}}\underline{p}$ with the half of the horizontal $\phi_{z,\text{camera}}^{\text{user}}$ and the half of the vertical $\phi_{y,\text{camera}}^{\text{user}}$ angle of view of the camera, respectively. Because the above transformation is not bijective and hence not invertible, the transformation of a point from the image to the local reference system requires a backprojection length d as additional information

$$T_{\mathbf{LI}} : \mathbb{R}_{\geq 0}, \mathbb{R}^2_{[-1,1]} \to \mathbb{R}^3$$

$$d, {}_{\mathbf{I}}\underline{p} = \begin{bmatrix} \mathbf{I}x \\ \mathbf{I}y \end{bmatrix} \mapsto \mathbf{L}\underline{p} = \begin{bmatrix} \mathbf{L}x \\ \mathbf{L}y \\ \mathbf{L}z \end{bmatrix} = d \begin{bmatrix} \cos\left({}_{\mathbf{L}}\phi_y\right) \\ \cos\left({}_{\mathbf{L}}\phi_y\right) \\ \sin\left({}_{\mathbf{L}}\phi_y\right) \end{bmatrix} \odot \begin{bmatrix} \cos\left({}_{\mathbf{L}}\phi_z\right) \\ \sin\left({}_{\mathbf{L}}\phi_z\right) \\ 1 \end{bmatrix}$$

$$\text{with } {}_{\mathbf{L}}\phi_z = -\frac{1}{2}\phi_{z,\text{camera}}^{\text{user}} \cdot {}_{\mathbf{I}}x, \ {}_{\mathbf{L}}\phi_y = \frac{1}{2}\phi_{y,\text{camera}}^{\text{user}} \cdot {}_{\mathbf{I}}y. \tag{3.12}$$

Note that $\odot$ denotes the Hadamard product , i.e., the element-wise product of two equally dimensioned matrices. In contrast to $T_{\mathbf{LG}}$ and $T_{\mathbf{GL}}$, the transformations between the local and the image reference system are not invertible. However, it is assumed that for the relevant points located within the field of view of the camera the transformations approximately invert each other

$$T_{\mathbf{LI}} \circ T_{\mathbf{IL}} \left({}_{\mathbf{L}}p \right) \approx {}_{\mathbf{L}}p, \quad T_{\mathbf{IL}} \circ T_{\mathbf{LI}} \left(d, {}_{\mathbf{I}}p \right) \approx {}_{\mathbf{I}}p. \tag{3.13}$$

Transformation between the global and the image reference system

The transformation of points between the global and the image reference frame are obtained by composing the transformations via the local reference system

$$T_{\mathbf{IG}} = T_{\mathbf{IL}} \circ T_{\mathbf{LG}} : \ \mathbb{R}^3 \to \mathbb{R}^2_{[-1,1]}$$
$$T_{\mathbf{GI}} = T_{\mathbf{GL}} \circ T_{\mathbf{LI}} : \ \mathbb{R}_{\geq 0}, \mathbb{R}^2_{[-1,1]} \to \mathbb{R}^3. \tag{3.14}$$

Since $T_{\mathbf{LG}}$ and $T_{\mathbf{GL}}$ are the inverse of each other and it is assumed that $T_{\mathbf{IL}}$ and $T_{\mathbf{IL}}$ approximately invert each other, the above compositions also approximately invert each other

$$T_{\mathbf{GI}} \circ T_{\mathbf{IG}} \left({}_{\mathbf{G}}p \right) \approx {}_{\mathbf{G}}p, \quad T_{\mathbf{IG}} \circ T_{\mathbf{GI}} \left(d, \ {}_{\mathbf{I}}p \right) \approx {}_{\mathbf{I}}p. \tag{3.15}$$

3.2 ANN module

The function of the ANN module is to make navigation decisions on the basis of the images from the onboard camera and other, user-switchable inputs. Fed to the planning module, these navigation decisions effectively lead the drone through the racetrack.

The current, preprocessed RGB image is a mandatory component of the input to the ANN module

$$\underline{\underline{I}}^{\mathrm{preproc}} \in \left\{ \frac{i}{I^{\mathrm{raw}}_{\mathrm{max}}} \right\}^{I_{\mathrm{C}} \times I^{\mathrm{preproc}}_{\mathrm{H}} \times I^{\mathrm{preproc}}_{\mathrm{W}}}_{i \in \{0, \dots, I^{\mathrm{raw}}_{\mathrm{max}}\}} \tag{3.16}$$

with the number of channels $I_{\mathrm{C}} = 3$ for RGB. The preprocessing of the raw RGB image entails two steps. First, the pixel intensities are normalized by the full intensity $I^{\mathrm{raw}}_{\mathrm{max}} = 255$ with the aim to accelerate the training of the ANN. Second, the image is sized down with a user-specied factor preserving its aspect ratio to the height $I^{\mathrm{preproc}}_{\mathrm{H}} = \left\lfloor s^{\mathrm{user}}_{\mathrm{rgb\text{-}resize}} \cdot I^{\mathrm{raw}}_{\mathrm{H}} \right\rfloor$ and width $I^{\mathrm{preproc}}_{\mathrm{W}} = \left\lfloor s^{\mathrm{user}}_{\mathrm{rgb\text{-}resize}} \cdot I^{\mathrm{raw}}_{\mathrm{W}} \right\rfloor$. By this, the occupation of GPU memory at the training of the ANN can be reduced if necessary.

In addition to the RGB image, the user may enable the current data of the onboard IMU

$$\left({}_{\mathbf{L}}\underline{a}^{\mathrm{imu}}, \ {}_{\mathbf{L}}\underline{\omega}^{\mathrm{imu}} \right) \tag{3.17}$$

as optional input component. The IMU data comprises the current measurements of the linear acceleration ${}_{\mathbf{L}}\underline{a}^{\mathrm{imu}} \in \mathbb{R}^3$ and the angular velocity ${}_{\mathbf{L}}\underline{\omega}^{\mathrm{imu}} \in \mathbb{R}^3$ of the drone with respect to the local reference system (see section XXX). Further optional components of the input are the durations Δt^{rgb} and Δt^{imu} elapsed between the previous and the current RGB image and IMU data, respectively.

In order to achieve a high degree of flexibility for potential studies, the ANN module itself is designed modularly from the CNN, the CAT, the GRU, the FC and the HEAD sub-modules (see figure XXX). While the sequence of these sub-modules cannot be changed, the user may individually switch on/off the inner sub-modules, i.e., the CAT,

the GRU and the FC. The outer sub-modules, i.e., the CNN and the HEAD, are mandatory, in order to ensure the mapping of the minimum input of an RGB image to an output.

CNN

The convolutional neural network (CNN) sub-module extracts a batch of visual features from the pixel data of a batch of images

$$\underline{\underline{\mathcal{F}}}^{\text{cnn}} : \mathbb{R}^{N^{\text{cnn}}_{\text{batch}} \times N^{\text{cnn}}_{\text{channel}} \times N^{\text{cnn}}_{\text{height}} \times N^{\text{cnn}}_{\text{width}}} \longrightarrow \mathbb{R}^{N^{\text{cnn}}_{\text{batch}} \times N^{\text{cnn}}_{\text{out}}}$$

$$\underline{\underline{x}} \mapsto \underline{\underline{\mathcal{F}}}^{\text{cnn}} \left(\underline{\underline{x}} \right). \tag{3.18}$$

The batch size $N^{\text{cnn}}_{\text{batch}}$, the number of channels $N^{\text{cnn}}_{\text{channel}}$ as well as the image height $N^{\text{cnn}}_{\text{height}}$ and width $N^{\text{cnn}}_{\text{width}}$ of the CNN adapt to the dimensions of the inputted batch of images $\underline{\underline{x}}$, whereas the output size $N^{\text{cnn}}_{\text{out}}$ of the CNN is fixed by the design of the CNN, more specifically, by its last layer. The training data is generally sequential, i.e., the images are present in batches of sequences

$$\underline{\underline{x}}^{\text{rgb}} \in \mathbb{R}^{N^{\text{batch}} \times N^{\text{seq}} \times N^{\text{C}} \times N^{\text{H}} \times N^{\text{W}}} \tag{3.19}$$

with the sequence lenght N^{seq}. These batches of sequences must be vectorized along their two first dimensions

$$\text{vec} \left(\underline{\underline{x}}^{\text{rgb}} \right) \in \mathbb{R}^{N^{\text{batch}} \cdot N^{\text{seq}} \times N^{\text{C}} \times N^{\text{H}} \times N^{\text{W}}} \tag{3.20}$$

before they are processed by the CNN. Afterwards the sequences are restored by devectorizing the direct output of the CNN backbone

$$\underline{\underline{x}}^{\text{cnn}} = \text{vec}^{-1} \left(\underline{\underline{\mathcal{F}}}^{\text{cnn}} \left(\text{vec} \left(\underline{\underline{x}}^{\text{rgb}} \right) \right) \right) \in \mathbb{R}^{N^{\text{batch}} \times N^{\text{seq}} \times N^{\text{cnn}}_{\text{out}}}. \tag{3.21}$$

CAT

The CAT sub-module concatenates each corresponding pair of sequential feature matrices, sampled from the batch outputted by the CNN sub-module and the batch of optional inputs, along their feature axis

$$\mathcal{F}^{\text{cat}} : \left(\mathbb{R}^{N^{\text{seq}} \times N^{\text{cnn}}_{\text{out}}}, \mathbb{R}^{N^{\text{seq}} \times N^{\text{input}}_{\text{opt}}} \right) \rightarrow \mathbb{R}^{N^{\text{seq}} \times \left(N^{\text{cnn}}_{\text{out}} + N^{\text{input}}_{\text{opt}} \right)}$$

$$\left(\underline{x}_i, \underline{y}_i \right) \mapsto \left[\underline{x}_i \quad \underline{y}_i \right], \qquad i \in \left\{ 1, \dots, N^{\text{batch}} \right\}. \tag{3.22}$$

If the user deactivates all optional input, i.e., $N_{\text{opt}}^{\text{input}} = 0$, the CAT sub-module recedes to the identity map of the output of the CNN sub-module. Either way, the CAT sub-module has zero trainable parameters

$$N_{\text{param}}^{\text{cat}} = 0. \tag{3.23}$$

GRU

The GRU sub-module consists of multiple layers of gated recurrent units (GRU) [3].

The input to a single unit is a batch of sequences of feature vectors

$$\left(\underline{x}_k \right)_{k \in \{1, \ldots, N^{\text{seq}}\}, j}, \quad j \in \left\{ 1, \ldots, N^{\text{batch}} \right\} \tag{3.24}$$

and a batch of the hidden states previously inferenced by the unit

$$\underline{h}_{0,j}, \quad j \in \left\{ 1, \ldots, N^{\text{batch}} \right\}. \tag{3.25}$$

___

The i-th gated recurrent unit maps the k-th feature vector of the j-th sequence of its input batch, i.e., $\underline{x}_{k,j}$, and the j-th previous hidden state of its hidden batch, i.e., $\underline{h}_{k-1,j}$, to the j-th current hidden state of its output batch, i.e., $\underline{h}_{k,j}$, by averaging its new gate $\mathcal{F}_{\text{new},i}^{\text{gru}}$ and its previous hidden state, weighted with its update gate $\mathcal{F}_{\text{upd},i}^{\text{gru}}$

$$\forall \quad i \in \{1, \ldots, N_{\text{unit}}^{\text{gru}}\}, \, j \in \{1, \ldots, N^{\text{batch}}\}, \, k \in \{1, \ldots, N^{\text{seq}}\}:$$
$$\mathcal{F}_{\text{hidden},i}^{\text{gru}} : \left(\mathbb{R}^{N_{\text{in},i}^{\text{gru}}}, \, [-1,1]^{N_{\text{hidden}}^{\text{gru}}} \right) \to [-1,1]^{N_{\text{hidden}}^{\text{gru}}}$$
$$\chi := \left(\underline{x}_{k,j}, \, \underline{h}_{k-1,j} \right) \mapsto$$
$$\underline{h}_{k,j} = \left[1 - \mathcal{F}_{\text{upd},i}^{\text{gru}} (\chi) \right] \odot \mathcal{F}_{\text{new},i}^{\text{gru}} (\chi) + \mathcal{F}_{\text{upd},i}^{\text{gru}} (\chi) \odot \underline{h}_{k-1,j}. \tag{3.26}$$

In addition to the update and new gate, a gated recurrent unit also incorporates the reset gate which is used to compute the new gate. These three gates follow the mappings

$$\forall \quad i \in \{1, \ldots, N_{\text{unit}}^{\text{gru}}\}, \, j \in \{1, \ldots, N^{\text{batch}}\}, \, k \in \{1, \ldots, N^{\text{seq}}\}:$$
$$\mathcal{F}_{\text{reset},i}^{\text{gru}}, \, \mathcal{F}_{\text{upd},i}^{\text{gru}}, \, \mathcal{F}_{\text{new},i}^{\text{gru}} : \left(\mathbb{R}^{N_{\text{in},i}^{\text{gru}}}, \, [-1,1]^{N_{\text{hidden}}^{\text{gru}}} \right) \to [0,1]^{N_{\text{hidden}}^{\text{gru}}}, \, [0,1]^{N_{\text{hidden}}^{\text{gru}}}, \, [-1,1]^{N_{\text{hidden}}^{\text{gru}}}$$
$$\chi := \left(\underline{x}_{k,j}, \, \underline{h}_{k-1,j} \right) \mapsto$$
$$\sigma \bigcirc \left(\underline{\underline{A}}_{x,i}^{\text{reset}} \underline{x}_{k,j} + \underline{b}_{x,i}^{\text{reset}} + \underline{\underline{A}}_{h,i}^{\text{reset}} \underline{h}_{k-1,j} + \underline{b}_{h,i}^{\text{reset}} \right),$$
$$\sigma \bigcirc \left(\underline{\underline{A}}_{x,i}^{\text{upd}} \underline{x}_{k,j} + \underline{b}_{x,i}^{\text{upd}} + \underline{\underline{A}}_{h,i}^{\text{upd}} \underline{h}_{k-1,j} + \underline{b}_{h,i}^{\text{upd}} \right),$$
$$\tanh \bigcirc \left[\underline{\underline{A}}_{x,i}^{\text{new}} \underline{x}_{k,j} + \underline{b}_{x,i}^{\text{new}} + \mathcal{F}_{\text{reset}}^{\text{gru}} (\chi) \odot \left(\underline{\underline{A}}_{h,i}^{\text{new}} \underline{h}_{k-1,j} + \underline{b}_{h,i}^{\text{new}} \right) \right]. \tag{3.27}$$

The reset gate linearly transforms the feature vector and the previous hidden state with the matrices of trainable weights and the vectors of trainable biases

$$\underline{\underline{A}}_{x,i}^{\text{reset}} \in \mathbb{R}^{N_{\text{hidden}}^{\text{gru}} \times N_{\text{in},i}^{\text{gru}}}, \qquad\qquad \underline{\underline{A}}_{h,i}^{\text{reset}} \in \mathbb{R}^{N_{\text{hidden}}^{\text{gru}} \times N_{\text{hidden}}^{\text{gru}}},$$
$$\underline{b}_{x,i}^{\text{reset}} \in \mathbb{R}^{N_{\text{hidden}}^{\text{gru}}}, \qquad\qquad \underline{b}_{h,i}^{\text{reset}} \in \mathbb{R}^{N_{\text{hidden}}^{\text{gru}}}, \tag{3.28}$$

and applies the standard sigmoid function [7]

$$\sigma: \ \mathbb{R} \to [0,1]\,; \ x \mapsto \frac{1}{1+e^{-x}} \tag{3.29}$$

elementwise (denoted with $\bigcirc$) to the result. The update gate differs to the reset gate only in the fact that it has own trainable weights and biases

$$\underline{\underline{A}}_{x,i}^{\text{upd}} \in \mathbb{R}^{N_{\text{hidden}}^{\text{gru}} \times N_{\text{in},i}^{\text{gru}}}, \qquad\qquad \underline{\underline{A}}_{h,i}^{\text{upd}} \in \mathbb{R}^{N_{\text{hidden}}^{\text{gru}} \times N_{\text{hidden}}^{\text{gru}}},$$
$$\underline{b}_{x,i}^{\text{upd}} \in \mathbb{R}^{N_{\text{hidden}}^{\text{gru}}}, \qquad\qquad \underline{b}_{h,i}^{\text{upd}} \in \mathbb{R}^{N_{\text{hidden}}^{\text{gru}}}. \tag{3.30}$$

The new gate also linearly transforms the feature vector and the previous hidden state with its own weights and biases

$$\underline{\underline{A}}_{x,i}^{\text{new}} \in \mathbb{R}^{N_{\text{hidden}}^{\text{gru}} \times N_{\text{in},i}^{\text{gru}}}, \qquad\qquad \underline{\underline{A}}_{h,i}^{\text{new}} \in \mathbb{R}^{N_{\text{hidden}}^{\text{gru}} \times N_{\text{hidden}}^{\text{gru}}},$$
$$\underline{b}_{x,i}^{\text{new}} \in \mathbb{R}^{N_{\text{hidden}}^{\text{gru}}}, \qquad\qquad \underline{b}_{h,i}^{\text{new}} \in \mathbb{R}^{N_{\text{hidden}}^{\text{gru}}}. \tag{3.31}$$

In contrast to the other two gates, the new gate, before building the sum of both linear transformations, mitigates the contribution of the linear transformation of the hidden state by the Hadamard product with the reset gate. Moreover, the hyperbolic tangent [20]

$$\tanh: \ \mathbb{R} \to [-1,1]\,; \ x \mapsto \frac{e^x - e^{-x}}{e^x + e^{-x}} \tag{3.32}$$

and not the sigmoid function is applied element-wise.

applies the following maps For the computation of the current batch of hidden states, the unit intermittently maps its input to three gates. The reset gate is computed by applying the sigmoid function $\sigma(x) = \frac{1}{1+\exp(-x)}$ to the individual elements of the sum of the biased linear transformations to the inputs and the previous hidden states and the subsequent

This multi-layer gated recurrent unit (GRU) uses feedback connection to process the time series data thereby inttroducing temporal understanding in the decision making.

FC

The FC sub-module comprises multiple fully connected layers applied to a batch of features. Each layer $i \in \left\{1, \ldots, N_{\text{layer}}^{\text{fc}}\right\}$ applies an activation function, a dropout and a

biased linear transformation on each element $j \in \left\{ 1, \dots, N^{\text{batch}} \right\}$ of a batch

$$\mathcal{F}_i^{\text{fc}} : \mathbb{R}^{N_{\text{in},i}^{\text{fc}}} \to \mathbb{R}^{N_{\text{out}}^{\text{fc}}}$$
$$\underline{x}_j \mapsto \underline{\underline{A}}_i^{\text{fc}} \left(\underline{\delta}^{\text{fc}} \odot f^{\text{fc}} \bigcirc \left(\underline{x}_j \right) \right) + \underline{b}_i^{\text{fc}}. \tag{3.33}$$

The activation function $f^{\text{fc}} : \mathbb{R} \to \mathbb{R}$ is applied element-wise (denoted with $\bigcirc$) on the input and is chosen by the user from the non-linear activations provided by PyTorch[1]. The dropout[8] decreases the overfitting of the ANN module on the training data set by enforcing the neurons to learn the detection of stand-alone features whose informative value is independent from the relation to other detected features. The dropout is accomplished by the Hadamard product (denoted with $\odot$) with the vector

$$\underline{\delta}^{\text{fc}} = \left[\delta_i^{\text{fc}} \right]_{i \in \left\{ 1, \dots, N_{\text{in},i}^{\text{fc}} \right\}} \tag{3.34}$$

of independent, scaled Bernoulli random variables that are resampled for every function call with the probabilities

$$P \left(\delta_i^{\text{fc}} = 0 \right) = p^{\text{fc}}, \quad P \left(\delta_i^{\text{fc}} = \frac{1}{1 - p^{\text{fc}}} \right) = 1 - p^{\text{fc}}. \tag{3.35}$$

During training, the dropout probability $p^{\text{fc}} \in [0, 1]$ equates to value specified by the user, whereas during evaluation, it is null $p^{\text{fc}} = 0$ whereby the dropout becomes an identity operation. The linear transformation consist of the linear map given by the matrix of trainable weights

$$\underline{\underline{A}}_i^{\text{fc}} \in \mathbb{R}^{N_{\text{in},i}^{\text{fc}} \times N_{\text{out}}^{\text{fc}}} \tag{3.36}$$

and the addition of the vector of trainable biases

$$\underline{b}_i^{\text{fc}} \in \mathbb{R}^{N_{\text{out}}^{\text{fc}}}. \tag{3.37}$$

A single layer, thus, has $\left(N_{\text{in},i}^{\text{fc}} + 1 \right) \cdot N_{\text{out}}^{\text{fc}}$ trainable parameters. The user specifies the number of layers $N_{\text{layer}}^{\text{fc}}$ of the FC, the width $N_{\text{out}}^{\text{fc}}$, i.e., the number of outputted features, which is shared by all layers of the FC, the activation function $f^{\text{fc}} : \mathbb{R} \to \mathbb{R}$ and the dropout probability $p^{\text{fc}} \in [0, 1]$. The number of inputted features of a layer adapts to the given input $N_{\text{in},i}^{\text{fc}} = \begin{cases} \dim \left(\underline{x}_j \right), & \text{if } i = 1 \\ N_{\text{out}}^{\text{fc}}, & \text{else} \end{cases}$. For $N_{\text{layer}}^{\text{fc}} \geq 1$, the FC sub-module hence has a total of $\left(N_{\text{in},i}^{\text{fc}} + 1 \right) N_{\text{out}}^{\text{fc}} + \left(N_{\text{layer}}^{\text{fc}} - 1 \right) \left(N_{\text{out}}^{\text{fc}} + 1 \right) N_{\text{out}}^{\text{fc}}$ trainable parameters.

---

[1] https://pytorch.org/docs/stable/nn.html, visited on 03/07/2022

HEAD

The HEAD sub-module is mandatory since it produces the final output of the entire ANN module which is, depending on the user's selection, either a navigation decision or a control command. A navigation decision

$$\left(v_{\text{norm}}, \; {}_{\text{I}}\underline{p}^{\text{wayp}}\right) \tag{3.38}$$

consists of a normalized speed $v_{\text{norm}} \in [0, 1]$ and a waypoint ${}_{\text{I}}\underline{p}^{\text{wayp}} \in [-1, 1]^2$ in the image reference system (see figure 3.1b). A control command

$$\left({}_{\text{I}}\underline{\omega}^{\text{cmd}}, \; {}_{\text{I}}\underline{\dot{\omega}}^{\text{cmd}}, \; c^{\text{cmd}}\right) \tag{3.39}$$

comprises the desired angular velocity ${}_{\text{I}}\underline{\omega}^{\text{cmd}}$ (also referred to as body rates) and acceleration ${}_{\text{I}}\underline{\dot{\omega}}^{\text{cmd}}$ of the drone body as well as the desired collective thrust c^{drone} of the drone rotors. In the limited scope of this master's thesis, the option to output control commands is only implemented but not tested in experiments. The mapping of the HEAD entails an activation function and a biased linear transformation which are deployed to each feature vector of the input batch

$$\mathcal{F}^{\text{head}} : \mathbb{R}^{N_{\text{in}}^{\text{head}}} \to \mathbb{R}^{N_{\text{out}}^{\text{head}}}$$
$$\underline{x}_j \mapsto \underline{\underline{A}}^{\text{head}} \left(f^{\text{head}} \bigcirc \left(\underline{x}_j\right)\right) + \underline{b}^{\text{head}}, \quad j \in \left\{1, \ldots, N^{\text{batch}}\right\}. \tag{3.40}$$

This structure is similar to a layer of the FC sub-module (see equation 3.33), leaving out the dropout functionality. While the number of input features is adaptive

$$N_{\text{in}}^{\text{head}} = \dim\left(\underline{x}_j\right), \tag{3.41}$$

the number of output features is determined by the user-selected output

$$N_{\text{out}}^{\text{head}} = \begin{cases} 3, & \text{if navigation decision} \\ 7, & \text{if control command} \end{cases}. \tag{3.42}$$

The total number of trainable parameters of the HEAD sub-module is

$$N_{\text{params}}^{\text{head}} = \left(N_{\text{in}}^{\text{head}} + 1\right) N_{\text{out}}^{\text{head}} \tag{3.43}$$

3.2.1 Baseline config

-resize image dims by a factor -cnn backbone -cat cnn output with optional inputs -multilayer gru if data sequential -multilayer fc -head

Output

3.3 Planning module

The task of the planning module is to translate the current navigation decision

$$\left(\tilde{v}_{\text{des}}^{\text{d}}, \; {}_{\mathbf{I}}\underline{p}^{\text{wp}}\right) \tag{3.44}$$

into a local trajectory that leads the drone to the position indicated by ${}_{\mathbf{I}}\underline{p}^{\text{wp}}$ with a speed depending on $\tilde{v}_{\text{des}}^{\text{d}}$. While at testing, the navigation decisions are exclusively made by the ANN module (see equation 3.38), at training, individual decisions may have been corrected by the expert system (see equation 3.55). Besides the current navigation decision, the planning module additionally requires the input of the current state of the drone comprising the position, the velocity and the acceleration

$$\mathbf{G}\underline{p}^{\text{d}}, \; \mathbf{G}\underline{v}^{\text{d}}, \; \mathbf{G}\underline{a}^{\text{d}}. \tag{3.45}$$

The drone state either corresponds to the ground-truth state in simulation or, in real-world, is obtained by a state estimation system.

First, the normalized, desired speed component of the navigation decision is rescaled

$$v_{\text{des}}^{\text{d}} = \max\left(\breve{v}_{\text{min}}^{\text{d}}, \quad \breve{v}_{\text{max}}^{\text{d}} \cdot \tilde{v}_{\text{des}}^{\text{d}}\right) \tag{3.46}$$

with the user-specified minimum $\breve{v}_{\text{min}}^{\text{d}}$ and maximum speed $\breve{v}_{\text{max}}^{\text{d}}$. Second, the waypoint component of the navigation decision is transformed according to equation 3.14 from the image to the global reference system

$$\mathbf{G}\underline{p}^{\text{wp}} = T_{\mathbf{GI}}\left(d^{\text{d-wp}}, \; {}_{\mathbf{I}}\underline{p}^{\text{wp}}\right). \tag{3.47}$$

Thereby, the distance $d^{\text{d-wp}}$ from the drone to the waypoint is used as the backprojection length in equation 3.12. The distance is computed by integrating the rescaled speed over the duration $\breve{t}_{\triangle}^{\text{d-wp}}$

$$d^{\text{d-wp}} = \max\left(\breve{d}_{\text{min}}^{\text{d-wp}}, \quad \min\left(v_{\text{des}}^{\text{d}} \cdot \breve{t}_{\triangle}^{\text{d-wp}}, \quad \breve{d}_{\text{max}}^{\text{d-wp}}\right)\right) \tag{3.48}$$

with the user-specified minimum $\breve{d}_{\text{min}}^{\text{d-wp}}$ and maximum distance $\breve{d}_{\text{max}}^{\text{d-wp}}$. Third, the local trajectory

$$\mathbf{G}\underline{p}^{\text{lt}} : \mathbb{R}_{[0, t_{\triangle}^{\text{lt}}]} \to \mathbb{R}^3; \quad t \mapsto \mathbf{G}\underline{p}^{\text{lt}}(t) \tag{3.49}$$

from the current drone state to the waypoint is generated according to the algorithm of Mueller et. al. [17] which minimizes the jerk of the trajectory

$$\min \int_0^{t_\Delta^{\mathrm{lt}}} \left\| {}_{\mathbf{G}}\dddot{\underline{p}}^{\mathrm{lt}}(t) \right\|_2^2 \mathrm{d}t$$
$$\text{s.t.} \quad {}_{\mathbf{G}}\underline{p}^{\mathrm{lt}}(0) = {}_{\mathbf{G}}\underline{p}^{\mathrm{d}} \qquad {}_{\mathbf{G}}\underline{p}^{\mathrm{lt}}(t_\Delta^{\mathrm{lt}}) = {}_{\mathbf{G}}\underline{p}^{\mathrm{wp}}$$
$$\phantom{\text{s.t.} \quad} {}_{\mathbf{G}}\dot{\underline{p}}^{\mathrm{lt}}(0) = {}_{\mathbf{G}}\underline{v}^{\mathrm{d}} \qquad {}_{\mathbf{G}}\dot{\underline{p}}^{\mathrm{lt}}(t_\Delta^{\mathrm{lt}}) \text{ free}$$
$$\phantom{\text{s.t.} \quad} {}_{\mathbf{G}}\ddot{\underline{p}}^{\mathrm{lt}}(0) = {}_{\mathbf{G}}\underline{a}^{\mathrm{d}} \qquad {}_{\mathbf{G}}\ddot{\underline{p}}^{\mathrm{lt}}(t_\Delta^{\mathrm{lt}}) \text{ free.} \tag{3.50}$$

The above optimization problem is computed in closed solution, which was derived with Pontryagin's maximum principle. Further, the dynamic constraints of the drone are only taken into account at a subsequent feasibility check. Thus, the algorithm is characterized by a low computational complexity and can be executed at the higher frequencies required by the navigation method of this thesis. The duration of the local trajectory is given by the quotient of the distance from the drone to the waypoint and the average speed of the trajectory

$$t_\Delta^{\mathrm{lt}} = \frac{d^{\mathrm{d\text{-}wp}}}{v_{\mathrm{avg}}^{\mathrm{lt}}}. \tag{3.51}$$

The average speed is yielded by upper-bounding the denormalized speed by the current speed of the drone plus a user-specified maximum speed increment

$$v_{\mathrm{avg}}^{\mathrm{lt}} = \min \left(v_{\mathrm{des}}^{\mathrm{d}}, \quad \left\| {}_{\mathbf{G}}\underline{v}^{\mathrm{d}} \right\|_2 + \breve{v}_\Delta^{\mathrm{d}} \right) \tag{3.52}$$

in order to prevent too steep speed increases.

3.4 Control module

Publish reference state from local trajectory to autopilot

$$t^{\mathrm{loctraj}} = t - t_0^{\mathrm{loctraj}} + T^{\mathrm{mainloop}} \tag{3.53}$$

Sample reference state

$$\underline{p}^{\mathrm{ref}} = \underline{p}^{\mathrm{loctraj}}(t^{\mathrm{loctraj}}), \ \dots, \ \underline{j}^{\mathrm{ref}} = \underline{j}^{\mathrm{loctraj}}(t^{\mathrm{loctraj}}), \ \phi_z^{\mathrm{ref}} = \mathrm{atan2}\left(v_y^{\mathrm{loctraj}}(t^{\mathrm{loctraj}}), v_x^{\mathrm{loctraj}}(t^{\mathrm{loctraj}}) \right) \tag{3.54}$$

track the ref states -¿ lo2w level control commands control scheme by Faessler et al. [5]

Training data generation

3.5 Expert system

The training data for the ANN module is automatically generated. For this, a slightly extended version of the expert system by Kaufmann et al. [**?**] (they referred to it as expert policy) is implemented. In the context of machine learning, an expert system is a program that imitates a human expert in order to solve a **problem**. It comprises two main components: a **knowledge base** that stores known facts and rules, and an **inference engine** which, by applying the rules to the known facts, generates new facts [**?**].

Problem

At training data generation (see XXX), the expert system undertakes the task of the ANN module by either making navigation decisions

$$\left(v_{\text{norm}}, \; {}_{\text{I}}\underline{p}^{\text{wayp}} \right) \tag{3.55}$$

instead of the fully untrained ANN module or correcting the false navigation decisions of the partly trained ANN module.

Knowledge Base

The expert system makes navigation decisions on its knowledge base which consists of the following facts (**F***) and rules (**R***).

F1 Current drone position and orientation in the global reference frame

$$ {}_{\text{G}}\underline{p}^{\text{drone}} \in \mathbb{R}^3, \quad {}_{\text{G}}\underline{q}_{\text{drone}} \in \mathbb{R}^4. \tag{3.56}$$

In simulation, ${}_{\text{G}}\underline{p}^{\text{drone}}$ and ${}_{\text{G}}\underline{q}_{\text{drone}}$ comply with their ground-truth values, whereas in real-world experiments they can only be estimated.

F2 The center points of the gates, i.e., the waypoints of the racetrack, in the global reference system

$$\left({}_{\text{G}}\underline{p}_i^{\text{gate}} \in \mathbb{R}^3 \right)_{i \in \{0, ..., N^{\text{gate}} - 1\}} \tag{3.57}$$

as well as the initial index to the currently targeted gate

$$i_{\text{curr}} = i_{\text{curr}}^{\text{init}} \in \{0, ..., N^{\text{gate}} - 1\}. \tag{3.58}$$

F3 Positions and velocities in the global reference frame from the sampled states of the global trajectory, i.e., the previously computed minimum-snap trajectory [?] traversing through the center points of the gates

$$\left({}_{\mathbf{G}}\underline{p}_i^{\mathrm{traj}} \in \mathbb{R}^3 \right)_{i \in \{0,...,N^{\mathrm{traj}}-1\}}, \quad \left({}_{\mathbf{G}}\underline{v}_i^{\mathrm{traj}} \in \mathbb{R}^3 \right)_{i \in \{0,...,N^{\mathrm{traj}}-1\}}. \tag{3.59}$$

R1 If the drone is closer to the currently targeted gate than a user-specified distance

$$\left\| {}_{\mathbf{G}}\underline{p}_{i_{\mathrm{curr}}}^{\mathrm{gate}} - {}_{\mathbf{G}}\underline{p}^{\mathrm{drone}} \right\|_2 < d_{\mathrm{drone\text{-}curr}}^{\mathrm{user}}, \tag{3.60}$$

increment the index to the currently targeted gate

$$i_{\mathrm{curr}} \leftarrow (i_{\mathrm{curr}} + 1) \bmod N^{\mathrm{gate}}. \tag{3.61}$$

R2 Update the index $i_{\mathrm{proj}} \in \{0, ..., N^{\mathrm{traj}} - 1\}$ to the projection state, i.e., the state of the global trajectory onto which the current drone position is projected, with the following iterative method.

1. Decrement the index to the projection state to compute the index to the previous state of the global trajectory

$$i_{\mathrm{prev}} = (i_{\mathrm{proj}} - 1 + N^{\mathrm{traj}}) \bmod N^{\mathrm{traj}}. \tag{3.62}$$

2. Starting from the previous state, compute the vector to the projection state

$$_{\mathbf{G}}\underline{a} = {}_{\mathbf{G}}\underline{p}_{i_{\mathrm{proj}}}^{\mathrm{traj}} - {}_{\mathbf{G}}\underline{p}_{i_{\mathrm{prev}}}^{\mathrm{traj}} \tag{3.63}$$

and the vector to the current drone position

$$_{\mathbf{G}}\underline{b} = {}_{\mathbf{G}}\underline{p}^{\mathrm{drone}} - {}_{\mathbf{G}}\underline{p}_{i_{\mathrm{prev}}}^{\mathrm{traj}}. \tag{3.64}$$

3. If the scalar product of the vectors $_{\mathbf{G}}\underline{a}$ and $_{\mathbf{G}}\underline{b}$, both normalized by the length of $_{\mathbf{G}}\underline{a}$, is less than 1

$$\frac{_{\mathbf{G}}\underline{a}^T {}_{\mathbf{G}}\underline{b}}{_{\mathbf{G}}\underline{a}^T {}_{\mathbf{G}}\underline{a}} < 1, \tag{3.65}$$

go to the next step. Else, increment the index to the projection state

$$i_{\mathrm{proj}} \leftarrow (i_{\mathrm{proj}} + 1) \bmod N^{\mathrm{traj}} \tag{3.66}$$

and go back to step 1.

4. If the drone is within a user-specified distance to the projection state

$$\left\| {}_{\mathbf{G}}\underline{p}^{\text{drone}} - {}_{\mathbf{G}}\underline{p}^{\text{traj}}_{i_{\text{proj}}} \right\|_2 \leq d^{\text{user}}_{\text{drone-proj}}, \tag{3.67}$$

the index i_{proj} to the projection state is found. Else, set the index to the state of the global trajectory which has the minimum distance to the current drone position

$$\underset{i_{\text{proj}}}{\arg\min} \left\| {}_{\mathbf{G}}\underline{p}^{\text{drone}} - {}_{\mathbf{G}}\underline{p}^{\text{traj}}_{i_{\text{proj}}} \right\|_2. \tag{3.68}$$

Due to this step, the expert system does not require to know the initial index $j^{\text{init}}_{\text{proj}} \in \{0, ..., N_{\text{traj}} - 1\}$ to the projection state.

Figure 3.2 schematically illustrates the above method with a 2D example.

R3 Update the index $i_{\text{speed}} \in \{0, ..., N^{\text{traj}} - 1\}$ to the speed state, i.e., the state of the global trajectory that is the basis for the normalized speed v_{norm} decision, by iteratively finding the first state of the global trajectory that follows the projection state with a specific distance.

1. Initialize the searched index with the index to the projection state

$$i_{\text{speed}} = i_{\text{proj}}. \tag{3.69}$$

2. Increment the searched index

$$i_{\text{speed}} \leftarrow (i_{\text{speed}} + 1) \bmod N^{\text{traj}}. \tag{3.70}$$

3. If the speed state is further from the projection state than a user-specified distance

$$\left\| {}_{\mathbf{G}}\underline{p}^{\text{traj}}_{i_{\text{speed}}} - {}_{\mathbf{G}}\underline{p}^{\text{traj}}_{i_{\text{proj}}} \right\|_2 > d^{\text{user}}_{\text{proj-speed}}. \tag{3.71}$$

the searched index is found. Else, go back to step 2.

R4 Update the index $i_{\text{wayp}} \in \{0, ..., N^{\text{traj}} - 1\}$ to the waypoint state, i.e., the state of the global trajectory that is the basis for the image waypoint ${}_{\mathbf{I}}\underline{p}^{\text{wayp}}$ decision, by iteratively finding the first state of the global trajectory that follows the projection state with a specific distance.

1. Set the distance from the projection state to the waypoint state by choosing the shorter distance from the drone to either the currently targeted gate or the lastly targeted gate, however, it must be greater than a user-specified distance

$$d_{\text{proj-wayp}} = \max \left\{ d^{\text{user}}_{\text{proj-wayp, min}}, \min \left\{ \begin{matrix} \left\| {}_{\mathbf{G}}\underline{p}^{\text{gate}}_{i_{\text{last}}} - {}_{\mathbf{G}}\underline{p}^{\text{drone}} \right\|_2, \\ \left\| {}_{\mathbf{G}}\underline{p}^{\text{gate}}_{i_{\text{curr}}} - {}_{\mathbf{G}}\underline{p}^{\text{drone}} \right\|_2 \end{matrix} \right\} \right\}. \tag{3.72}$$
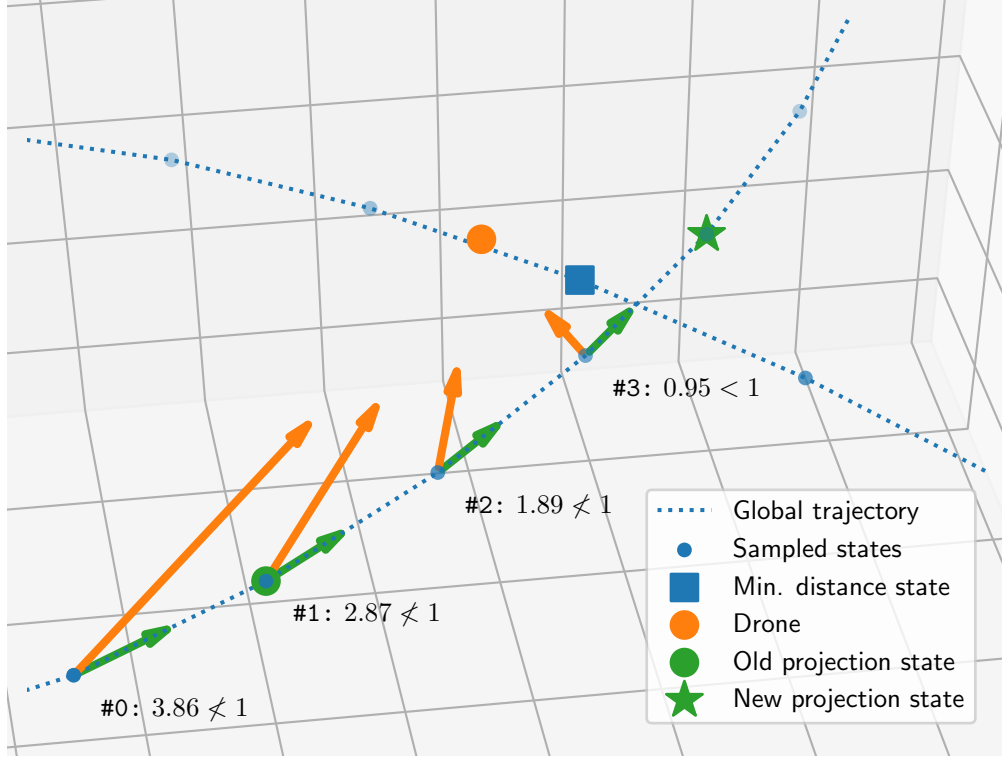
31

Figure 3.2: Schematic 2D example of the iterative method to update the index to the projection state.

The positions of the states (blue points) sampled from the global trajectory (blue dotted line), the old index to the projection state (green circle) and the current position of the drone (orange circle) are known. At each iteration of the method, the vector from the previous state to the projection state (green arrows, equation 3.63) and the vector from the previous state to the drone position (orange arrows, equation 3.64) are computed. Then, the normalized dot product criterion (annotations, equation 3.65) is checked. For iteration #0-2, the criterion is not fullfilled. Thus, the index to the projection state is incremented and another iteration is started. At iteration #3 the criterion is finally met and the new index to the projection state (green star) is identified - assuming the distance criterion (equation 3.67) is also true. Note that finding the index to the projection state only with the minimum distance criterion (equation 3.68) would have failed here, since the state that is closest to the drone (blue square) belongs to a later or earlier part of the global trajectory which intersects the current part.

2. Initialize the searched index with the index to the projection state

$$i_{\text{wayp}} = i_{\text{proj}}. \tag{3.73}$$

3. Increment the searched index

$$i_{\text{wayp}} \leftarrow (i_{\text{wayp}} + 1) \bmod N^{\text{traj}}. \tag{3.74}$$

4. If the waypoint state is further from the projection state than the distance computed in step 1

$$\left\| \mathbf{G}\underline{p}_{i_{\text{wayp}}}^{\text{traj}} - \mathbf{G}\underline{p}_{i_{\text{proj}}}^{\text{traj}} \right\|_2 > d_{\text{proj-wayp}}, \tag{3.75}$$

the searched index is found. Else, go back to step 3.

R4 Compute the normalized speed decision as the Frobenius norm of the velocity at the speed state normalized by the maximum speed of all states of the global trajectory

$$v_{\text{norm}} = \frac{\left\| \mathbf{G}\underline{v}_{i_{\text{speed}}}^{\text{traj}} \right\|_2}{\underset{i}{\text{argmax}} \left\| \mathbf{G}\underline{v}_{i}^{\text{traj}} \right\|_2} \in [0, 1]. \tag{3.76}$$

R4 Compute the image waypoint decision by transforming the waypoint state from the global via the local to the image reference system

$$_{\mathbf{I}}\underline{p}^{\text{wayp}} = T_{\mathbf{IL}} \left(T_{\mathbf{LG}} \left(\mathbf{G}\underline{p}_{i_{\text{wayp}}}^{\text{traj}} \right) \right) \in \mathbb{R}^2. \tag{3.77}$$

Inference Engine

- Implemented as a set of functions within a C++ ros node, that fetches the known facts via ROS topics or computes and store them as internal variables.

- The user can de-/activate the expert system as functional part of the navigation method.

is build and send to the planning module as input. In addition, it is used as label for the current training sample. The features of the training samples are ... .

3.6 Training procedure

3.7 Test procedure

Chapter 4

Experiments

4.1   Simulation environment

4.2   Test designs

4.3

Chapter 5

Evaluation

DELETEME: The evaluation chapter is one of the most important chapters of your work. Here, you will prove usability/efficiency of your approach by presenting and interpreting your results. You should discuss your results and interprete them, if possible. Drawing conclusions on the results will be one important point that your estimators will refer to when grading your work.

5.1 Results

5.2 Discussions

Chapter 6

Conclusion and Future Work

6.1 Summary

DELETEME: put a plain summary of your work here. Summaries should be made of each Chapter beginning with Chapter 2 and ending with you evaluation. Just write down what you did and describe the corresponding results without reflecting on them.

6.2 Conclusion

DELETEME: do not summarize here. Reflect on the results that you have achieved. What might be the reasons and meanings of these? Did you make improvements in comparison to the state of the art? What are the good points about your results and work? What are the drawbacks?

6.3 Future Work

DELETEME: Regarding your results - which problems did you not solve? Which questions are still open? Which new questions arised? How should someone / would you continue working in your thesis field basing on your results?

- `https://en.wikipedia.org/wiki/Gated_recurrent_unit#Content-Adaptive_Recurrent_Unit`

- `https://en.wikipedia.org/wiki/Gated_recurrent_unit#Architecture`

Bibliography

[1] Y. Bengio, P. Simard, and P. Frasconi. Learning long-term dependencies with gradient descent is difficult. *IEEE Transactions on Neural Networks*, 5(2):157–166, mar 1994.

[2] Mike Brookes. The matrix reference manual. 2020. URL: `http://www.ee.imperial.ac.uk/hp/staff/dmb/matrix/intro.html` (accessed on 08/07/2022).

[3] Kyunghyun Cho, Bart van Merrienboer, Dzmitry Bahdanau, and Yoshua Bengio. On the properties of neural machine translation: Encoder-decoder approaches. September 2014.

[4] Junyoung Chung, Caglar Gulcehre, KyungHyun Cho, and Yoshua Bengio. Empirical evaluation of gated recurrent neural networks on sequence modeling, 2014.

[5] Mikel L. Forcada and Rafael C. Carrasco. Learning the initial state of a second-order recurrent neural network during regular-language inference. *Neural Computation*, 7(5):923–930, sep 1995.

[6] Klaus Greff, Rupesh K. Srivastava, Jan Koutnik, Bas R. Steunebrink, and Jurgen Schmidhuber. LSTM: A search space odyssey. *IEEE Transactions on Neural Networks and Learning Systems*, 28(10):2222–2232, oct 2017.

[7] Jun Han and Claudio Moraga. The influence of the sigmoid function parameters on the speed of backpropagation learning. In *Lecture Notes in Computer Science*, pages 195–201. Springer Berlin Heidelberg, 1995.

[8] Geoffrey E. Hinton, Nitish Srivastava, Alex Krizhevsky, Ilya Sutskever, and Ruslan R. Salakhutdinov. Improving neural networks by preventing co-adaptation of feature detectors. July 2012.

[9] Sepp Hochreiter. Untersuchungen zu dynamischen neuronalen netzen. *Diploma, Technische Universität München*, 91(1), 1991.

[10] Sepp Hochreiter and Jürgen Schmidhuber. Long short-term memory. *Neural Computation*, 9(8):1735–1780, nov 1997.

[11] Xiaolin Hu and P. Balasubramaniam. *Recurrent neural networks*. InTech, 2008.

[12] IBM Cloud Education. Recurrent neural networks. *IBM Cloud Learn Hub*, 2020. URL: `https://www.ibm.com/cloud/learn/recurrent-neural-networks` (accessed on 04/07/2022).

[13] Lukasz Kaiser and Ilya Sutskever. Neural gpus learn algorithms, 2015.

[14] Erik Learned-Miller. Vector, matrix, and tensor derivatives. URL: `http://cs231n.stanford.edu/vecDerivs.pdf` (accessed on 08/07/2022).

[15] Minchen Li. A tutorial on backward propagation through time (bptt) in the gated recurrent unit (gru) rnn. *Dept. Comput. Sci., Univ. British Columbia, Vancouver, BC, Canada, Tech. Rep*, 2016.

[16] Ali A. Minai and Ronald D. Williams. On the derivatives of the sigmoid. *Neural Networks*, 6(6):845–853, jan 1993.

[17] Mark W. Mueller, Markus Hehn, and Raffaello D'Andrea. A computationally efficient algorithm for state-to-state quadrocopter trajectory generation and feasibility verification. pages 3480–3486, Tokyo, Japan, 2013. IEEE.

[18] Razvan Pascanu, Tomas Mikolov, and Yoshua Bengio. On the difficulty of training recurrent neural networks. In *International conference on machine learning*, pages 1310–1318. PMLR, 2013.

[19] Raúl Rojas. The backpropagation algorithm. In *Neural Networks*, pages 149–182. Springer Berlin Heidelberg, 1996.

[20] D. S., Milton Abramowitz, and Irene A. Stegun. Handbook of mathematical functions with formulas, graphs, and mathematical tables. *Mathematics of Computation*, 20(93):167, jan 1966.

[21] Jürgen Schmidhuber. The most cited neural networks all build on work done in my labs. *Jürgen Schmidhuber's AI Blog*, 2021. URL: `https://people.idsia.ch/~juergen/most-cited-neural-nets.html` (accessed on 04/07/2022).

[22] Wenpeng Yin, Katharina Kann, Mo Yu, and Hinrich Schütze. Comparative study of cnn and rnn for natural language processing, 2017.

[23] Hans-Georg Zimmermann, Christoph Tietz, and Ralph Grothmann. Forecasting with recurrent neural networks: 12 tricks. In *Lecture Notes in Computer Science*, pages 687–707. Springer Berlin Heidelberg, 2012.

Appendices

DELETEME: everything that does not fit into your work, e.g. a 5 page table that breaks the reading flow, should be placed here

Appendix A: Abbreviations

AES   Advanced Encryption Standard (Symmetrisches Verschlüsselungsverfahren)
ASCII   American Standard Code for Information Interchange (Computer-Textstandard)
dpi   dots per intch (Punkte pro Zoll; Maß für Auflösung von Bilddateien)
HTML   Hypertext Markup Language (Textbasierte Webbeschreibungssprache)
JAP   Java Anon Proxy
JPEG   Joint Photographic Experts Group (Grafikformat)
JPG   Joint Photographic Experts Group (Grafikformat; Kurzform)
LED   Light Emitting Diode (lichtemittierende Diode)
LSB   Least Significant Bit
MD5   Message Digest (Kryptographisches Fingerabdruckverfahren)
MPEG   Moving Picture Experts Group (Video- einschließlich Audiokompression)
MP3   MPEG-1 Audio Layer 3 (Audiokompressionformat)
PACS   Picture Archiving and Communication Systems
PNG   Portable Network Graphics (Grafikformat)
RSA   Rivest, Shamir, Adleman (asymmetrisches Verschlüsselungsverfahren)
SHA1   Security Hash Algorithm (Kryptographisches Fingerabdruckverfahren)
WAV   Waveform Audio Format (Audiokompressionsformat von Microsoft)

Appendix B: LaTeX Help

How to Use This Template

- Remove all of my text which is mostly labeled with DELETEME

- Change the information in the 00a_title_page.tex file

- Use the information written in this section

- Ask you supervizor to help you

- If I am not your supervizor and noone else can help you, write me an email (aubrey.schmidt@dai-labor.de)

Citations

Citing is one of the essential points you need to do in you thesis. Statements not basing on results of your own research[1] not being cited represent a breach on the rules of scientific working. Therefore, you every statement needs to be cited basing on information that other people can cross-check. A common way of citing in technical papers is:

- Oberheide et al. [?] state that the average time for an anti-virus enginge to be updated with a signature to detect an unknown threat is 48 days.

Note: et al. is used when the paper was written by more than two people. Check the code of this section to learn how to cite from a technical perspective.

Note: you can change the citation style in the `thesis.tex` file, e.g. to harvard style citations. Instructions on this can also be found in this file.

You should not cite anything that can be changed, e.g. it is not that good citing web pages since they might get updated changing the cited content. There are no clear quality measures on citing sources but aubrey believes that the following list is true for several cases, starting with highest quality:

1. Journal article or book

2. Conference paper

3. Workshop paper

4. Technical report

5. Master thesis

---

[1]in what ever context

6. Bachelor thesis

7. General Web reference

There might be workshop papers that have a higher quality than some journal papers. Therefore this list only gives you a hint on possible quality measures. Another measure can be whether a paper was indexed by ACM/IEEE, although this is not a strong indicator.

Finding and Handling Citation Sources

Following ressources are required for finding and handling articles, books, papers and sources.

- your primary resource will be `http://scholar.google.com`

- `http://www.google.com` might also be used

- `wikipedia.com` can be a good start for finding relevant papers on your topic

- you should download and install JabRef or a similar tool `http://jabref.sourceforge.net/`

- you should point JabRef to the mybib.bib file

- you should immediately enter a relevant paper to JabRef, additionally, you should write a short summary on it; else, you will do this work at least twice.

General Advices

- Do not take care of design, LaTeXwill do this for you. If you still feel that you need to take care of this, do this when you have finished writing, else you will end up in a lot of double and triple work.

- LaTeXwill do exactly that you will tell it to do. If you have problems with this, go for google or ask you supervizor

- use labels in order to be able to reference to chapters, section, subsections, figures, tables, etc. ...

General Commands

- check `http://en.wikibooks.org/wiki/LaTeX`

- check `http://www.uni-giessen.de/hrz/tex/cookbook/cookbook.html` German

Please also check the following source [**?**].

Code

This section shows you how to get your code into a LaTeXdocument. See code for options.

```
1  class Beispiel{
2
3    public static void main(String args[]){
4
5       System.out.println("Hello_World");
6
7    }
8
9  }
```

```
1 class Beispiel{
2
3   public static void main(String args[]){
4
5      System.out.println("Hello World");
6
7   }
8
9 }
```

Listing 6.1: Example code is presented here

Figures

This section describes how to include images to your document. Information was taken from `http://en.wikibooks.org/wiki/LaTeX/Floats,_Figures_and_Captions`, visited on 05/08/2011. Please make sure to use original vector graphics as basis since image quality might be used as weak indicator for thesis quality. For this, try to find find files in `.SVG` or `.PDF` format. Exporting a `.PNG` or `.JPG` to `.PDF` will not work since data was already lost while exporting it to these formats. This is the case for most Web graphics. Wikipedia startet entering most in images in `.SVG` which easily can be transformed to `.PDF`, but please do not forget proper citations.

Figure 6.1: Including an image; in this case a PDF. Please note that the caption is placed below the image.

Figure 6.2: See code for caption options: this is a long caption which is printed in the Text. Additionally, image size was increased

(a) Small   (b) Large   (c) Medium

Figure 6.3: Placing images side by side using the subfig package. Space between the images can be adjusted.

Tables

Here, you will find some example tables.The tables were taken from `http://en.wikibooks.org/wiki/LaTeX/Tables`, visited on 05/08/2011. Table environment was added plus caption and label. For code, check `__help/latex_hinweise.tex`.

Table 6.1: Simple table using vertical lines. Note that the caption is always above the table! Please check code for finding the right place for the table label.

1	2	3
4	5	6
7	8	9

Table 6.2: Table using vertical and horizontal lines

7C0	hexadecimal
3700	octal
11111000000	binary
1984	decimal

Table 6.3: Table with column width specification on last column

Day	Min Temp	Max Temp	Summary
Monday	11C	22C	A clear day with lots of sunshine. However, the strong breeze will bring down the temperatures.
Tuesday	9C	19C	Cloudy with rain, across many northern regions. Clear spells across most of Scotland and Northern Ireland, but rain reaching the far northwest.

Table 6.4: Table using multi-column and multirow

Team sheet		
Goalkeeper	GK	Paul Robinson
Defenders	LB	Lucus Radebe
	DC	Michael Duberry
	DC	Dominic Matteo
	RB	Didier Domi
Midfielders	MC	David Batty
	MC	Eirik Bakke
	MC	Jody Morris
Forward	FW	Jamie McMaster
Strikers	ST	Alan Smith
	ST	Mark Viduka